Journal of Medicinal Chemistry

Article

Targeting the Binding Function 3 (BF3) Site of the Androgen Receptor Through Virtual Screening. 2. Development of 2-((2-phenoxyethyl) thio)-1H-benzimidazole derivatives.

Ravi Sashi Nayana Munuganti, Eric Leblanc, Peter Axerio-Cilies, Christophe Labriere, Kate Frewin, Kriti Singh, Mohamed DH Hassona, Nathan A Lack, Huifang Li, Fuqiang Ban, Emma Guns, Robert Young, Paul S Rennie, and Artem Cherkasov

J. Med. Chem., **Just Accepted Manuscript** • DOI: 10.1021/jm3015712 • Publication Date (Web): 09 Jan 2013

Just Accepted

Targeting the Binding Function 3 (BF3) Site of the Androgen Receptor Through Virtual Screening. 2. Development of 2-((2-phenoxyethyl) thio)-1H-benzimidazole derivatives.

M. Ravi Shashi Nayana,[a,1] Eric Leblanc,[a,1] Peter Axerio-Cilies,[a] Christophe Labriere,[b] Kate Frewin,[a] Kriti Singh [a], Mohamed D.H. Hassona,[a] Nathan A. Lack,[c] Huifang Li,[a] Fuqiang Ban,[a,*] Emma Tomlinson Guns,[a] Robert Young, [b] Paul S. Rennie,[a, 2] and Artem Cherkasov [a,,2]

[a] Vancouver Prostate Centre, University of British Columbia, 2660 Oak Street, Vancouver, British Columbia V6H 3Z6, Canada

[b] Department of Chemistry, Simon Fraser University, 8888, University Drive, Burnaby, British Columbia, V5A 1S6, Canada

[c] Koç University School of Medicine, Istanbul, Turkey

1 Authors contributed equally to this work

2 Dr. Cherkasov's and Dr. Rennie's labs made equal contributions to this work.

** Telephone: 604-875-4111. Fax: 604-875-5654. E-mail: fban@prostatecentre.com*

PDB ID: 4HLW

ABSTRACT

The human androgen receptor (AR) is a proven therapeutic target in prostate cancer. All current anti-androgens, such as Bicalutamide, Flutamide, Nilutamide and Enzalutamide, target the buried hydrophobic androgen binding pocket of this protein. However, effective resistance mechanisms against these therapeutics exist, such as mutations occurring at the target site. To overcome these limitations, the surface pocket of the AR called Binding Function 3 (BF3) was characterised as an alternative target for small molecule therapeutics. A number of AR inhibitors directly targeting the BF3 were previously identified by us (*J. Med. Chem.* 2011, 54, 8563). In the current study, based on the prior results, we have developed structure-activity-relationships that allowed designing a series of 2-((2-phenoxyethyl) thio)-1H-benzimidazole and 2-((2-phenoxyethyl) thio)-1H-indole as lead BF3 inhibitors. Some of the developed BF3 ligands demonstrated significant anti-androgen potency against LNCaP and Enzalutamide-resistant prostate cancer cell lines.

INTRODUCTION

The androgen receptor (AR) plays a pivotal role in the development of the prostate gland as well as is involved in occurrence and progression of prostate cancer (PCa).[1] It has also been observed that the AR is overexpressed in the majority of castration-resistant prostate cancers (CRPCs).[2, 3] With recurrent or metastatic PCa, the first line of treatment is some form of androgen withdrawal therapy that blocks either the production of androgens or their binding to the AR.[4, 5] Unfortunately the effectiveness of this approach is usually temporary due to progression of surviving tumor cells to the castration resistant state. [6]

The currently existing anti-androgens, such as Bicalutamide, Flutamide, Nilutamide, Enzalutamide (formerly known as MDV3100)[7] and experimental ARN509,[8] have essentially the same mechanism of action on the AR. Specifically, they all bind to its androgen binding site (ABS) resulting in conformational changes of the receptor that prevent its activation.[7, 9] While these antagonists suppress the initial cancer growth, they become less effective with long-term therapy. One of the major causes of resistance is mutations in the ABS. Such mutations not only weaken AR-drug interactions, but may also turn antagonists into agonists, thereby promoting cancer progression. [10] Thus, there is an urgent need for novel therapeutic strategies to modulate AR, such as direct disruption of its critical interactions with co-activator proteins, mediated by Activation Function 2 (AF2) and Binding Function 3 (BF3) surface sites.

The AF2 is a hydrophobic groove formed on the surface of AR upon androgen binding. The recruitment of co-regulators at that site is critical for AR-regulated gene expression.[11] Thus, the AF2 pocket has been previously characterized as a suitable target site on the AR surface.[12-15] In a recent work, Fletterick *et al* identified an additional surface area adjacent to AF2 groove called the Binding Function 3 (BF3).[16] It has been proposed that the BF3 site can allosterically

affect the AF2 site and is implicated in the receptor's interaction with a FKPB52 protein – an important AR activator.[17] AF2 and BF3 surface pockets are likely to form an allosteric network that regulates AR LBD function and represent promising therapeutic targets.[18]

Previously, we conducted a large scale virtual screen against AF2 and BF3 sites. AR inhibitors of several chemical scaffolds that target the BF3 site were discovered and demonstrated anti-AR activity in the sub-micromolar range.[19] A comparison of the four reported co-crystal structures of the selected BF3 inhibitors revealed that residues of BF3 site may undergo significant conformational changes upon ligand binding. On the basis of the elucidated structure-activity-relationship of our virtual screening hits and binding poses in the co-crystals, 2-((2-phenoxyethyl)thio)-1H-benzo[d]imidazole was derived and proposed as a proper starting point for further ligand optimization.

In the present study, we are report on computer-aided design, synthesis and experimental evaluation of 2-((2-phenoxyethyl) thio)-1H-benzo[d]imidazole derivatives and 2-((2-phenoxyethyl) thio)-1H-indole derivatives as promising new BF3-directed inhibitors of the AR representing a potentially novel type of drugs for treating some forms of the CRPCs.

RESULTS

Identification of Analogs of Compound 1 by 2D Similarity Search Method: In the previous work, our group reported several small molecules that specifically target the AR-BF3 pocket.[19] Among them, (2-((2-phenoxyethyl) thio)-1-(2-(p-tolyloxy) ethyl)-1H-benzo[d]imidazole) derivative (compound **1)** was selected as a lead candidate. A chemical template was designed based on the structure of **1** (Figure 1) and a molecular similarity search was performed to identify compounds with different substitutions at R_1 and 1-5 positions of the

benzene ring of **1**. Instant JChem,[20] a 2D similarity searching tool from ChemAxon, was employed to search through ZINC database 12.0.[21] All software parameters were set to their default values. A total of 30 ZINC compounds which generated Tanimoto coefficient above 0.6 with respect to the query structure were selected and tested for their anti-AR activity (compounds **2-31** in Table 1).

Cell-Based Testing and *In Vitro* Characterization: The selected compounds were screened for their ability to inhibit AR transcriptional activity using a nondestructive, cell-based enhanced green fluorescent protein (eGFP) AR transcriptional assay [22] (see Materials and Methods). In this assay, the expression of eGFP is under the direct control of an androgen responsive probasin-derived promoter and enables quantification of AR transcriptional activity. 13 of the purchased compounds exhibited >50% inhibition of AR transcription at a concentration of 50μM. These were subjected to concentration-dependent titration to establish corresponding IC_{50} values (Table 1). The observed IC_{50} values were estimated to be in the range of 11-60μM. These inhibitors were then tested in SRC2-3 peptide and androgen displacement assays for their ability to displace SRC2 peptide from the AF2 site and androgen from the ABS, respectively. None of the compounds were active in these assays, confirming that they target the BF3 pocket. From the cell proliferation assay, the compounds were also confirmed to be nontoxic to non-AR containing cells at a 50μM concentration administered for over 72h (data not shown).

Since the molecules selected from the 2D similarity search did not result in compounds with improved cell-based activity, the lead optimization was initiated.

Rational Design, Synthesis and Characterization of 2-((2-phenoxyethyl) thio)-1H-benzimidazole: Based on the crystallographically determined binding pose of a compound **1** (2YLO) and the corresponding activity profiles of their analogues, we hypothesized that solvent-

exposed substituents at the R_1 position of the ligands are not likely to contribute to target affinity. To test this hypothesis, we designed a compound **32** where R_1 = H (Table 1). The structure was built using the MOE program and energy minimization was performed by applying the MMFF94X force field. The compound was then docked into the AR crystal structure (2YLO structure) using the Glide SP program without applying any constraints. From the docking pose, we could observe that compound **32** is anchored to the protein site by a hydrogen bond that it forms with the Glu837 side chain. Compound **32** was synthesized and evaluated by the eGFP transcriptional assay. As anticipated, it exhibited approximately a 3-fold increase (IC_{50}=4.2μM) of AR transcriptional activity inhibition compared to the parent substance (IC_{50}=13.1μM). The dose-response curve for compound **32** is presented on Figure 2A.

Furthermore, we have tested compound **32** with the AF2 peptide displacement assay and androgen displacement assay where it did not demonstrate any detectible levels if activity, confirming that it is a specific BF3 binder. Biolayer interferometry (BLI) studies demonstrated a direct reversible interaction between this compound and AR LBD (Figure 2B).

Based on these observations, we concluded that the formation of H-bond between NH of the benzoimidazole moiety of compound **32** and the side chain of the Glu837 residue is a significant factor for protein-ligand affinity. This observation becomes particularly obvious when compound **32** is compared with the synthetic analogues **33**, **34**, **35** and **36,** which were designed and tested as negative probes and which also received lower docking scores due to the loss of a critical H-bond with Glu837. Upon testing for anti-AR activity, all these derivatives except compound **33** turned out to be completely inactive whereas compound **33** showed a 3-fold decrease in activity (IC_{50}=12μM) in the eGFP assay (compounds **33-36** in Table 1). Similarly, replacing benzoimidazole ring with benzoxazole, as in the case of compound **37,** caused a drastic

effect in activity and binding to the AR LBD. Since compound **32** has a promising experimental activity profile, it was subjected to structural elucidation using x-ray crystallography.

Crystallographic Structure of AR in Complex with 2-((2-phenoxyethyl) thio)-1H-benzimidazole: In an effort to unambiguously confirm the site of the compound's interaction, x-ray crystallographic studies were conducted with the AR and compound **32**. Following optimization of the soaking protocol, the structure of the AR in complex with compound **32** was determined to 2.5Å resolution. The crystallographic data refinement statistics for the corresponding PDB entry 4HLW are presented in Table 2. In the present crystallographic data set, there was clear electron density observed at the BF3 site, supporting the presence of the inhibitor. Interestingly, unlike the cases of previously published BF3 binders, such as compound A,[19] compound B (TRIAC), C (T3), and D (FLUF)[16] (Figure 1 in the supplementary data), compound **32** was found to reside specifically in the BF3 site. Since the crystallographic information is in agreement with the activity data, compound **32** could be characterized as a specific BF3 inhibitor. Figure 3A shows a good structural fit of compound **32** inside the target cavity. Notably, the experimentally determined configuration of the BF3-bound molecule is similar to its docking predicted pose generated by Glide (r.m.s.d=0.62Å), which gave confidence to rely on the adopted *in silico* protocol (Figure 2 in supplementary data).

The BF3 pocket is located on the AR surface close to the AF2 site. Since the AR androgen binding site is distant from the BF3 site, mutations that usually weaken interactions between the ABS and the current drugs should not affect the BF3-directed inhibitors. As it can be observed from the x-ray structure, the BF3 pocket is formed by residues from several LBD-forming helices. The residues contributing to BF3 formation are: Gln670, Pro671, Ile672 and Phe673 from the NH2-terminal part of a helix 1 (H1), Pro723, Gly724, Arg726 and Asn727 from

H3 and Phe826, Glu829, Leu830, Asn833, Glu837, and Arg840 from H9. The residues Arg726 and Asn727 act as boundary between the AF2 and BF3 sites and may play an important role in their cross talk and coordinated action.

The structure of the AR-LBD in complex with compound **32** is generally similar to the previously reported structures 2YLO. Compound **1** differs slightly in terms of its positioning inside the BF3. Thus, as predicted compound **32** forms a strong hydrogen bond between the NH benzimidazole moiety and side-chain carboxyl of the Glu837. Moreover, this compound maintains strong hydrophobic contacts with the neighboring residues, including Ile672, Phe673 and Leu830. Additional stabilization of the protein-ligand complex occurs due to T-shaped arene-arene conjugation between the phenyl ring of compound **32** and the Phe826 side chain. These interactions possibly explain the increased potency of compound **32** (IC_{50} =4.2μM) compared to its parental compound **1** as well as other structural analogues listed in Table 1 (where the corresponding IC_{50} values range from 11μM to >200μM). Since compound **32** demonstrated improved AR inhibitory activity profile and could be experimentally resolved inside the BF3 site, it was advanced into further optimization studies.

Structure Activity Relationship (SAR) for 2-((2-phenoxyethyl) thio)-1H-benzimidazole as AR BF3 ligands: To further explore the relevance of various structural elements of compound **32**, we designed 8 close derivatives of this compound by substituting its sulfur and oxygen atoms in the linker region (Table 3). Data obtained from Bio-Layer Interferometry (BLI) experiments and eGFP cellular assays revealed that subtle changes in the linker can have profound effects on target binding and inhibitory activity. Accordingly, we investigated the significance of a sulfur atom in compound **32** by replacing it with nitrogen (compound **38**) and carbon (compound **39**). These modifications abolished the cellular activity of

derivatives **38** and **39** and their binding to the AR. Similarly, the replacement of sulfur with sulfinyl and sulfonyl fragments caused a significant drop in activity of the corresponding derivatives **40** and **41**. The loss in activity of compounds **40** and **41** was due to the presence of oxygen which disrupts the critical Van der Waals contacts with Phe673, Tyr834 of the BF3 pocket. Our investigation then focused on oxygen atom of linker region in compound **32**. In particular, the replacement of oxygen with carbon resulted in compound **42**, which demonstrated a 4-fold drop in anti-AR potential (12μM). Surprisingly, replacing oxygen with nitrogen (compound **43**) exhibited detrimental effects on its binding and activity. Increasing the length of the linker fragment from SC_2H_4O to SC_3H_6O resulted in loss of activity of a derivative **44**, likely caused by its poor fit inside BF3. Shortening the linker region (*i.e.* removing oxygen atom and exchanging the SC_2H_4OPh fragment to SC_3H_6Ph) did not result in any major alteration of anti-AR potential, with the corresponding IC_{50} assessed for compound **45** at 7.4μM.

Another focal point of the study was evaluation of the effect of substitutions at the benzene ring of compound **32** (Table 4). The starting three analogues, **46**, **47** and **48,** were designed and synthesized by introducing a methyl group at R_1, R_2 and R_3 positions of the core. As predicted, compound **47** showed a 2-fold increase in AR-suppressing activity (IC_{50}=1.8μM) compared to the parental compound **32** whereas compound **46** demonstrated 5-fold decrease while compound **48** demonstrated only slightly lowered activity (IC_{50}=7.0μM). As our docking models demonstrated, the presence of a methyl group at the meta- position ensures additional hydrophobic contacts with the Phe826 and Leu830 residue of BF3 and contributing towards enhanced ligand binding (Figure 3 in Supplemental data). Similarly, 2, 5-methyl substitution was well-tolerated and led to further enhanced activity of the corresponding derivative **49** (IC_{50}=2.7μM). The dose response curve for compounds **47** and **49** is presented in Figure 4A. The

BLI experiment confirmed a direct reversible interaction between compounds **47**, **49** and the AR (see Figure 4B and 4C). We have also explored the introduction of chlorine atom into R_2 (compound **50**) and R_3 (compound **51**) substitution positions, which appear not to affect the overall activity. A larger sulfonamide group was not tolerated at position R_3 (**52**) and caused a 15-fold decrease in the inhibition activity.

An effort was also made to replace imidazole with an indole moiety in the developed BF3 inhibitors. Initially, we have made an indole-based compound **53** which demonstrated a similar level of AR inhibition compared to compound **32** with a corresponding IC_{50} of 5.4μM. Derivative **54** was designed by adding a sulfonamide group to the 7-position of compound **53**. According to the docking model, sulfonamide forms additional networks of hydrogen bonds with nearby residues (*i.e.* side chain of Arg840, Glu837, Asn833 and backbone of Pro671 (Figure 3B)). As a result, the compound demonstrated 4-fold increase its in activity (Figures 4A). The direct reversible interaction between this compound and the AR LBD was also detected by the BLI (Figure 4D). Based on the above observations, compounds **32**, **47**, **49** and **54** were selected for further evaluation.

Derivatives 32, 47, 49 and 54 Reduce PSA Expression in LNCaP and Enzalutamide-Resistant Cells: To rule out possible false positive hits in the AR transcriptional eGFP assay, we validated the activity of compounds **32**, **47**, **49** and **54** by quantifying their effect on the production of the prostate specific antigen (PSA) in prostate cancers cell lines.[23] PSA is a serine protease whose expression is dependent on AR activity level in the cell. PSA is widely used as a marker for PCa as its serum concentration is associated with this pathological condition. As expected, these derivatives induced a dose-dependent decrease in PSA levels in LNCaP prostate cancer cells [24] with corresponding IC_{50s} value determined as 4.3, 3.3, 1.9 and 1.6μM respectively

(Figure 5A). These compounds were also evaluated using *in house* developed Enzalutamide-resistant prostate cancer cells (Hidetoshi Kuruma *et al. Submitted to cancer research*, **2012**). These AR inhibitors are significantly more effective than Casodex and Enzalutamide in these cells. Figure 5B demonstrates that anti-AR drugs are ineffective, with IC_{50}s greater than 100μM. On the other hand, even though compound **32** (IC_{50}=21μM) reduced PSA levels moderately, derivatives **47**, **49** and **54** (IC_{50}=13, 6.8 and 6.4μM) were quite effective in these Enzalutamide resistant cells. Hence, the inhibition values obtained for inhibition of PSA in LNCaP and Enzalutamide-resistant cells confirms the effectiveness of these inhibitors on the AR signaling pathway.

Derivatives 32, 47, 49 and 54 Reduces Cell Growth in LNCaP and Enzalutamide-Resistant Cells: To ascertain the growth inhibitory potential of AR inhibitors **32**, **47**, **49** and **54**, we evaluated their ability to inhibit growth of LNCaP[24] and Enzalutamide-resistant prostate cancer cells, as well as on AR-independent PC3 cells. The cell viability was assessed after 4 days of incubation with the test compounds at a concentration of 6μM. Figure 6 shows that compound **32** did not have any significant inhibition effect on these cancer cells whereas its derivatives **47**, **49** and **54** suppress cancer cells quite effectively at the concentration measured. Derivatives **49** and **54** exhibit a particularly strong effect on the growth of both LNCaP and Enzalutamide-resistant cells. Moreover, derivatives **47**, **49** and **54** did not show any effect on AR independent PC3 cell lines, confirming their AR-specific activity.

Derivatives 32, 47, 49 and 54 are Selective AR BF3 inhibitors: We undertook to profile the selectivity of these derivatives for AR over estrogen receptor α (ER-α), the other member of the steroidal nuclear receptor subfamily. The compounds were tested for their ability to inhibit 17β-Estradiol (E2)-ERα-mediated gene transcription in MCF-7 human breast cancer

cells using luciferase reporter whose expression is driven by consensus estrogen response element. Supplementary Figure 4 shows that the compounds do not inhibit ER-α transcriptional activity compared to Tamoxifen (Tx) measured at 3 different concentrations (10, 5 and 1μM). This confirms that these inhibitors are AR-BF3 specific.

DISCUSSION

Surface pockets or protein-protein interaction sites are often considered as attractive opportunities for therapeutic targeting. However, identifying small molecules that modulate these sites is often difficult owing to issues such as lack of a well-defined deep binding pocket. Although surface sites are challenging drug targets, their adaptive character can provide binding grooves for compounds and thus opportunities for drug discovery.[25, 26] In the case of the AR, targeting its BF3 pocket offers a promising alternative strategy to create novel therapeutics for castration-resistant prostate cancer. Since the AR BF3 is surface exposed, identifying compounds with significant activity profiles and developing structure activity relationship around them is challenging.

We have previously utilized the power of virtual screening combined with experimental evaluations to discover a number of small molecules that effectively target the BF3 site of the AR. On the basis of one of the identified inhibitors (compound **1**), we developed a series of analogues with improved anti-AR activity. In particular, a simplified yet more active derivative **32** was synthesized, experimentally evaluated and crystallographically resolved inside the AR BF3 target cavity. The reported structure 4HLW demonstrated that benzimidazole moiety of the parent compound **32** makes a strong H-bond with neighboring residue Glu837. The information obtained by both inhibition experiments and x-ray crystallography studies indicated that

compound **32** is a strong BF3-specific inhibitor. Hence, we synthesized a number of derivatives of this compound and explored their structure-activity relationship in the context of anti-AR potency**.**

We initially modified the linker region of compound **32**. Replacement of the oxygen atom in SC_2H_4O was tolerated, but did not result in further improvement of potency. Other modifications completely abolished anti-AR activity and binding. Hence, we focused on introducing groups at the benzene ring of the compound **32** template.

By comparison, addition of small hydrophobic substituents such as methyl at various position of the benzene ring was able to enhance anti-AR potency of the corresponding derivatives of compound **32**. In particular, compounds **47** and **49**, containing methyl at meta- and di-ortho positions, demonstrated IC_{50} in single digit μ-molar range. Replacement of the benzoimidazole moiety in compound **32** with a synthetically more favorable indole fragment did not significantly alter the activity of the derivatives. The introduction of a sulfonamide group at 7-position of the indole core (compound **54**) further increased the target affinity by providing additional hydrogen bonds with Arg840 and Phe673 residues.

These findings culminated in the discovery of rather potent AR inhibitors **32**, **47**, **49** and **54** with the corresponding IC50s of 4.2, 1.8, 2.7 and 1.5μM respectively, which are 5-10 times lower than the IC_{50} of 13.1μM for the parental compound **1**. The activity of these chemicals was further confirmed by their ability to decrease the levels of PSA in LNCaP and Enzalutamide-resistant PCa cells. Compounds **32**, **47**, **49** and **54** exhibited IC_{50}s of 4.3, 1.9, 3.3 and 1.6μM respectively in LNCaP cells. Similar potencies were also observed in Enzalutamide-resistant cell line. Compounds **49** (IC_{50}=6.8μM) and **54** (IC_{50}=6.4μM) turned out to be especially effective in

comparison with clinically used Casodex and Enzalutamide (IC_{50}>100μM in these resistant cells). The PSA inhibition figures were also in agreement with the above numbers giving further confidence in these BF3 inhibitor prototypes.

In summary, while we obtained 30 analogues of compound **1** by 2D similarity search, they were not very active. However, when we rationally developed, synthesized and tested 21 benzimidazole derivatives of compounds **1** and 9 of them showed equivalent or improved potency against the AR. Similarly, we created and evaluated two indole derivatives which also exhibited enhanced anti-AR potency. These initial results obtained with indole-based compounds are encouraging and will be further investigated. Moreover, the structure of the AR in complex with compound **32** (one of the synthetic derivatives) was elucidated and turned out to be in very good agreement with our prior predictions, providing additional confidence in our modeling approach.

Drug resistance remains a fundamental cause of therapeutic failure in cancer therapy.[27, 28] In PCa, cancer progression to a drug-resistant phenotype in the presence of an antagonist possibly through selection of cells with epigenetics or mutational changes that bypass the inhibitory action of the drug. Our lead derivatives were tested for their ability to inhibit AR in LNCaP PCa cell lines including those which have developed resistance to the recently approved potent anti-androgen, Enzalutamide.[7] Results from cell viability assays indicated that the tested derivatives exhibited effective inhibition of growth in both LNCaP and Enzalutamide-resistant cell lines. There was no significant effect on the growth of PC3 PCa cells which lack the AR. The effectiveness of these BF3 inhibitors was also confirmed when they were shown to reduce the endogenous expression levels of PSA in Enzalutamide-resistant cell lines. Even though the specific mechanism for Enzalutamide-resistance in these cells is still unclear and may or may not

be fully related to mutations in the AR, the effectiveness of compounds **47**, **49** and **54** in these Enzalutamide-resistant cells substantiates targeting an alternative binding site on the AR such as the BF3. The results obtained from the ER-α luciferase assay confirm that these inhibitors are specific to AR and do not affect ER-α in human breast cancer cells.

In summary, we have developed a novel class of anti-AR drugs chemo-types with an alternative mechanism of action which can overcome conventional anti-androgen resistance and exhibit strong antagonism in PCa cell lines. These BF3 drugs have the potential to provide a further line of treatment after failure of conventional anti-androgens and progression to castration resistance.

CONCLUSIONS

In the current study, a series of 2-((2-phenoxyethyl) thio)-1H-benzimidazole and 2-((2-phenoxyethyl)thio)-1H-indole derivatives were rationally designed, synthesized and evaluated for their ability to inhibit human AR – a primary drug target in PCa. Importantly, these drugs bind to a newly characterized target site on the AR called Binding Function 3 (BF3) and therefore, exhibit a new mechanism for inhibition of the AR. It is anticipated that these novel AR inhibitors provide an alternative therapeutic strategy that can be applied or complimentary to current anti-androgen treatments for PCa patients. Furthermore, these BF3 drugs can be used when resistance arises to conventional anti-androgen therapies. They may also be used in combination with current anti-androgens to possibly avoid or delay progression to castration resistance. Since the emergence of castration resistance is the lethal end stage of the disease, we anticipate that the proposed research will eventually have a substantial impact on patient survival.

MATERIALS AND METHODS

2-[(2-phenoxyethyl)thio]-1*H*-benzimidazole (32): To a mixture of 1H-benzimidazole-2-thiol (0.50 g, 3.33 mmol, 1.0 eq.), K_2CO_3 (0.93 g, 6.66 mmol, 2.0 eq.) and TBAI (0.37g, 1.00 mmol, 0.3 eq.) in acetonitrile (20mL) was added (2-bromoethoxy)benzene (2.15 g, 9.99 mmol, 3.0 eq.). The reaction mixture was stirred at 35°C (oil bath at 40°C) during 16 h and then filtered and evaporated under reduced pressure. The residue was purified by silica gel flash-column chromatography (eluent: heptane/EtOAc, 90/10 to 70/30) to afford compound **32** (530 mg, 59 %) as a white solid. Note: A less polar compound was also isolated (370mg, 28%) and corresponds to the bis-alkylated derivative (characterization not included). **^{1}H NMR (DMSO, 400 MHz):** δ (ppm): 3.68 (2H, t, $J_{9'-8'}$= 6.4 Hz, 2H9'), 4.32 (2H, t, $J_{8'-9'}$= 6.4 Hz, 2H8'), 6.94 (1H, t, $J_{4'-3'}$= $J_{4'-5'}$= 7.4 Hz, H4'), 6.99 (2H, dm, $J_{2'-3'}$= $J_{6'-5'}$= 8.2 Hz, H2' & H6'), 7.11 to 7.15 (2H, m, H5 & H6), 7.29 (2H, tm, $J_{3'-2'}$= $J_{3'-4'}$= $J_{5'-6'}$= $J_{5'-4'}$= 7.4 Hz, H3' & H5'), 7.45 (2H, bs, H4 & H7) **^{13}C NMR (DMSO, 100 MHz):** δ (ppm): 30.7 (C9'), 66.8 (C8'), 110.9 (C7), 115.0 (C2' & C6'), 117.8 (C4), 121.3 (C4'), 121.9 (bs, C5 & C6), 130.0 (C3' & C5'), 150.2 (C2), 158.6 (C1') **MS:** ESI: m/z: 271.1 ($[M+H]^+$), 293.1 ($[M+Na]^+$) HRMS (ESI): calculated for $C_{15}H_{15}N_2OS$: m/z = 271.0900, found: 271.0914 calculated for $C_{15}H_{14}N_2NaOS$: m/z = 293.0719, found: 293.0730.

1-ethyl-2-[(phenoxyethyl)thio]-1*H*-benzimidazole (33): To a mixture of compound **32** (200 mg, 0.74 mmol, 1.0 eq.), K_2CO_3 (206 mg, 1.48 mmol, 2.0 eq.) and TBAI (111 mg, 0.30 mmol, 0.4 eq.) in acetonitrile (10 mL) was added ethyl bromide (220 µL, 2.96 mmol, 4.0 eq.). The reaction mixture was stirred at 35°C (oil bath at 40°C) during 48 h and then filtered over silica gel pad and evaporated under reduced pressure. The residue was triturated with heptane and diethyl ether to afford compound **33** (160 mg, 72 %) as a beige solid. **^{1}H NMR (DMSO, 400 MHz):** δ (ppm): 1.29 (3H, J= 7.2 Hz, ethyl), 3.74 (2H, t, $J_{9'-8'}$= 6.4 Hz, 2H9'), 4.18 (2H, q, J=

7.2 Hz, ethyl), 4.34 (2H, $J_{8'-9'}$= 6.4 Hz, 2H8'), 6.94 (1H, t, $J_{4'-3'}$= $J_{4'-5'}$= 7.8 Hz, H4'), 7.00 (2H, dm, $J_{2'-3'}$= $J_{6'-5'}$= 7.8 Hz, H2' & H6'), 7.16 to 7.20 (2H, m, H5 & H6), 7.29 (2H, tm, $J_{3'-2'}$= $J_{3'-4'}$= $J_{5'-6'}$= $J_{5'-4'}$= 7.8 Hz, H3' & H5'), 7.52 & 7.58 (2H, d & d, H4 & H7) **^{13}C NMR (DMSO, 100 MHz):** δ (ppm): 14.4 (ethyl), 30.6 (C9'), 38.4 (ethyl), 66.1 (C8'), 109.4 (C7), 114.5 (C2' & C6'), 117.6 (C4), 120.8 (C4'), 121.4 & 121.5 (C5 & C6), 129.5 (C3' & C5'), 135.7 (C3a), 142.9 (C7a), 150.3 (C2), 158.0 (C1') **MS:** ESI: m/z: 299.1 ($[M+H]^+$) HRMS (ESI): calculated for $C_{17}H_{19}N_2OS$: m/z = 299.1213, found: 299.1205

2-{2-[(phenoxyethyl)thio]-1*H*-benzimidazo-1-yl}ethanol (34): To a mixture of compound **32** (2.0 g, 7.4 mmol, 1.0 eq.) and K_2CO_3 (2.3 g, 16.6 mmol, 2.3 eq.) in NMP (15 mL) was added 2-bromoethanol (1.2 mL, 17.7 mmol, 2.4 eq.). The reaction mixture was stirred at 70°C for 15 h, allowed to cool to room temperature and then, diluted with water. The mixture was extracted with ethyl acetate and methyl *tert*-butyl ether. The organic layer was dried over Na_2SO_4, evaporated under reduced pressure and the residue was purified by silica gel flash-column chromatography (eluent: heptane/EtOAc, 90/10 to 60/40) to afford compound **34** (1.1 g, 47 %) as a white solid. **^{1}H NMR (DMSO, 400 MHz):** δ (ppm): 3.70 (4H, m, CH_2), 4.19 (2H, t, J= 7.0 Hz, CH_2), 4.32 (2H, $J_{8'-9'}$= 6.4 Hz, 2H8'), 4.97 (1H, t, J= 7.0 Hz, OH), 6.94 (1H, t, $J_{4'-3'}$= $J_{4'-5'}$= 7.8 Hz, H4'), 7.00 (2H, dm, $J_{2'-3'}$= $J_{6'-5'}$= 7.8 Hz, H2' & H6'), 7.16 to 7.18 (2H, m, H5 & H6), 7.29 (2H, tm, $J_{3'-2'}$= $J_{3'-4'}$= $J_{5'-6'}$= $J_{5'-4'}$= 7.8 Hz, H3' & H5'), 7.49 & 7.56 (2H, d & d, H4 & H7) **^{13}C NMR (DMSO, 100 MHz):** δ (ppm): 30.6 (C9'), 46.4 (CH_2), 59.2 (CH_2), 66.2 (C8'), 109.9 (C7), 114.5 (C2' & C6'), 117.5 (C4), 120.8 (C4'), 121.3 & 121.4 (C5 & C6), 129.5 (C3' & C5'), 136.6 (C3a), 142.8 (C7a), 151.2 (C2), 158.0 (C1') **MS:** ESI: m/z: 315.1 ($[M+H]^+$) **HRMS (ESI):** calculated for $C_{17}H_{19}N_2O_2S$: m/z = 315.1162, found: 315.1161

3-{2-[(2-phenoxyethyl)thio]-1*H*-benzimidazol-1-yl}propanoic acid (35): To a mixture of 3-{2-[(2-phenoxyethyl)thio]methyl-1*H*-benzimidazol-1-yl}propanoate (450 mg, 1.21 mmol) in acetic acid (10mL) and water (10mL) was added a concentrated HCl solution (3 mL). The reaction mixture was stirred at 80°C during 5 h and then co-evaporated with heptane and toluene under reduced pressure. The residue was taken up in ethyl acetate and the organic layer was dried over Na_2SO_4 and evaporated to afford, after trituration with methyl *tert*-butyl ether, compound **35** (180 mg, 43 %) as a white solid. **^{1}H NMR (DMSO, 600 MHz):** δ (ppm): 2.75 (2H, d, $J_{2\text{-}3}$= 7.0 Hz, 2H2), 3.76 (2H, t, $J_{8''\text{-}9''}$= 6.4 Hz, 2H8''), 4.33 (2H, t, $J_{9''\text{-}8''}$= 6.4 Hz, 2H9''), 4.42 (2H, d, $J_{3\text{-}2}$= 7.0 Hz, 2H3), 6.92-6.95 (3H, m, H4'', H2'' & H6''), 7.24-7.30 (4H, m, H5', H6', H3'' & H5''), 7.61 (1H, m, H4), 7.64 (1H, m, H7). **^{13}C NMR (DMSO, 150 MHz):** δ (ppm): 32.0 (C2), 33.8 (C9''), 40.2 (C3), 66.7 (C8''), 110.9 (C4'), 114.9 (C2'' & C6"), 117.3 (C7'), 121.4 (C4''), 122.9 (C5' & C6'), 130.0 (C3'' & C5''), 135.7 (C7a'), 151.3 (C2'), 158.4 (C1''), 172.3 (C1). **MS:** ESI: m/z: 343.1 ($[M+H]^+$) HRMS (ESI): calculated for $C_{18}H_{19}N_2O_3S$: m/z = 343.1111, found: 343.1081

1-allyl-2-[(2-phenoxyethyl)thio]-1*H*-benzimidazole (36) : To a mixture of compound **32** (300 mg, 1.11 mmol, 1.0 eq.), K_2CO_3 (309 mg, 2.22 mmol, 2.0 eq.) and TBAI (328 mg, 0.88 mmol, 0.8 eq.) in acetonitrile (10 mL) was added allyl bromide (0.580mL, 6.66 mmol, 6.0 eq.). The reaction mixture was stirred at 35°C during 20 h and then, diluted with water and extracted with methyl *tert*-butyl ether. The organic layer was dried over Na_2SO_4, filtered through a silica gel pad and evaporated to afford compound **36** (330 mg, 96 %) as a white solid.**^{1}H NMR (DMSO, 400 MHz):** δ (ppm): 3.73 (2H, t, $J_{9'\text{-}8'}$= 6.4 Hz, 2H9'), 4.33 (2H, $J_{8'\text{-}9'}$= 6.4 Hz, 2H8'), 4.80 (2H, m, 2H8), 4.97 (1H, dm, J_{trans}= 17.2 Hz, H10), 5.17 (1H, dm, J_{cis}= 10.2 Hz, H10), 5.90-5.99 (1H, m, H9), 6.95 (1H, t, $J_{4'\text{-}3'}$= $J_{4'\text{-}5'}$= 7.4 Hz, H4'), 7.00 (2H, dm, $J_{2'\text{-}3'}$= $J_{6'\text{-}5'}$=

7.8 Hz, H2' & H6'), 7.17 to 7.20 (2H, m, H5 & H6), 7.17 to 7.20 (2H, m, H5 & H6), 7.29 (2H, tm, $J_{3'-2'}$= $J_{3'-4'}$= $J_{5'-6'}$= $J_{5'-4'}$= 7.4 Hz, H3' & H5'), 7.46 (1H, dm, H4), 7.60 (1H, dm, H7) **^{13}C NMR (DMSO, 100 MHz):** δ (ppm): 31.3 (C9'), 46.1 (C8), 66.6 (C8'), 110.2 (C7), 115.0 (C2' & C6'), 117.7 (C10), 118.2 (C4), 121.3 (C4'), 122.1 & 122.2 (C5 & C6), 130.0 (C3' & C5'), 132.7 (C9), 136.6 (C3a), 143.4 (C7a), 151.5 (C2), 158.5 (C1') **MS:** ESI: m/z: 311.1 ($[M+H]^+$) **HRMS (ESI):** calculated for $C_{18}H_{19}N_2OS$: m/z = 311.1213, found: 311.1185

2-[(2-phenoxyethyl)thio]-1,3-benzoxazole (37): To a mixture of 1,3-benzoxazole-2-thiol (1.0 g, 6.7 mmol, 1.0 eq.), K_2CO_3 (1.9 g, 13.4 mmol, 2.0 eq.) and TBAI (1.5 g, 4.0 mmol, 0.6 eq.) in acetonitrile (40 mL) was added (2-bromoethoxy)benzene (1.6 g, 8.0 mmol, 1.2 eq.). The reaction mixture was stirred at 35°C (oil bath at 40°C) during 24 h and then, diluted with water and extracted with ethyl acetate. The organic layer was dried over Na_2SO_4 and evaporated under reduced pressure. The crude was taken up in CH_2Cl_2 and heptane, filtered through a silica gel pad and eluted with methyl *tert*-butyl ether to afford, after removal of solvent, compound **37** (1.1 g, 61 %) as a red solid.**^{1}H NMR (DMSO, 400 MHz):** δ (ppm): 3.73 (2H, t, $J_{9'-8'}$= 6.4 Hz, 2H9'), 4.36 (2H, t, $J_{8'-9'}$= 6.4 Hz, 2H8'), 6.94 (1H, m, H4'), 6.96 (2H, m, H2' & H6'), 7.28 (2H, tm, $J_{3'-2'}$= $J_{3'-4'}$= $J_{5'-6'}$= $J_{5'-4'}$= 7.4 Hz, H3' & H5'), 7.32-7.35 (2H, m, H5 & H6), 7.6-7.67 (2H, m, H4 & H7). **^{13}C NMR (DMSO, 100 MHz):** δ (ppm): 30.9 (C9'), 65.7 (C8'), 110.2 (C7), 114.5 (C2' & C6'), 118.2 (C4), 120.9 (C4'), 124.3 & 124.6 (C5 & C6), 129.5 (C3' & C5'), 141.2 (C3a), 151.3 (C2), 157.9 (C1'), 164.0 (C7a). **MS:** ESI: m/z: 272.1 ($[M+H]^+$) HRMS (ESI): calculated for $C_{15}H_{14}NO_2S$: m/z = 272.0740, found: 272.0750

2-[(2-phenoxyethyl) sulfinyl]-1*H*-benzimidazole (40) and 2-[(2-phenoxyethyl) sulfonyl]-1*H*-benzimidazole (41): To a mixture of compound **32** (200 mg, 0.74 mmol, 1.0 eq.) in CH_2Cl_2 (20 mL) was added, at 0°C, *m*-CPBA (383 mg, 2.22 mmol, 3.0 eq.). The reaction

mixture was stirred at 0°C during 10 min and then, quenched with a saturated aqueous sodium sulfite solution. The mixture was stirred at room temperature for several minutes, the organic layer dried over Na_2SO_4 and the solvent removed under reduced pressure. The residue was purified by silica gel flash-column chromatography (eluent: heptane/EtOAc, 80/20 to 40/60) to afford compounds **40** (110 mg, 52 %) and **41** (80 mg, 36 %) as white solids. **Compound 40:** **^{1}H NMR (DMSO, 400 MHz):** δ (ppm): 3.68 (1H, m, 1H9'), 3.78 (1H, m, 1H9'), 4.39-4.47 (2H, m, 2H8'), 6.81 (2H, d, $J_{2''-3''}$= $J_{6''-5''}$= 8.2 Hz, H2' & H6'), 6.94 (1H, t, $J_{4'-3'}$= $J_{4'-5'}$= 8.2 Hz, H4'), 7.26 (2H, t, $J_{3'-2'}$= $J_{3'-4'}$= $J_{5'-4'}$= $J_{5'-6'}$= 8.2 Hz, H3' & H5'), 7.31-7.33 (2H, m, H5 & H6), 7.66 (2H, bs, H4 & H7), 13.57 (1H, s, benzimidazolic H) **^{13}C NMR (DMSO, 100 MHz):** δ (ppm): 53.7 (C9'), 63.2 (C8'), 114.9 (C2' & C6), 121.5 (C4'), 123.6 (C5 & C6), 130.0 (C3'' & C5''), 154.6 (C2), 158.1 (C1') **MS:** ESI: m/z: 287.1 ($[M+H]^+$), 309.1 ($[M+Na]^+$) **HRMS (ESI):** calculated for $C_{15}H_{15}N_2O_2S$: m/z = 287.0849, found: 287.0833 calculated for $C_{15}H_{14}N_2NaO_3S$: m/z = 309.0668, found: 309.0653 ESI: m/z: 285.1 ($[M-H]^-$) **HRMS (ESI):** calculated for $C_{15}H_{13}N_2O_2S$: m/z = 285.0703, found: 285.0676 **Compound 41:** **^{1}H NMR (DMSO, 400 MHz):** δ (ppm): 4.11 (2H, t, $J_{8'-9'}$= 5.4 Hz, 2H8'), 4.38 (2H, t, $J_{9'-8'}$= 5.4 Hz, 2H9'), 6.48 (2H, d, $J_{2''-3''}$= $J_{6''-5''}$= 8.2 Hz, H2' & H6'), 6.88 (1H, t, $J_{4'-3'}$= $J_{4'-5'}$= 8.2 Hz, H4'), 7.15 (2H, t, $J_{3'-2'}$= $J_{3'-4'}$= $J_{5'-4'}$= $J_{5'-6'}$= 8.2 Hz, H3' & H5'), 7.40-7.42 (2H, m, H5 & H6), 7.71 (2H, bs, H4 & H7) **^{13}C NMR (DMSO, 100 MHz):** δ (ppm): 54.6 (C9'), 61.9 (C8'), 114.6 (C2' & C6), 121.5 (C4'), 129.8 (C3'' & C5''), 157.7 (C1') **MS:** ESI: m/z: 303.1 ($[M+H]^+$) **HRMS (ESI):** calculated for $C_{15}H_{15}N_2O_3S$: m/z = 303.0798, found: 303.0780 ESI: m/z: 301.1 ($[M-H]^-$) HRMS (ESI): calculated for $C_{15}H_{13}N_2O_3S$: m/z = 301.0624, found: 301.0652

2-[(3-phenylpropyl)thio]-1*H*-benzimidazole (42): To a mixture of 1*H*-benzimidazole-2-thiol (200 mg, 1.33 mmol, 1.0 eq.), K_2CO_3 (370 mg, 2.66 mmol, 2.0 eq.) and TBAI (295 mg,

0.80 mmol, 0.6 eq.) in acetonitrile (6 mL) was added (3-bromopropyl)benzene (606 µL, 3.99 mmol, 3.0 eq.). The reaction mixture was stirred at 35°C (oil bath at 40°C) during 48 h and then, diluted with water and extracted with ethyl acetate. The organic layer was dried over Na_2SO_4, evaporated under reduced pressure and the residue was purified by silica gel flash-column chromatography (eluent: heptane/EtOAc, 90/10 to 70/30) to afford compound **42** (260 mg, 73 %) as a white solid. Note: A less polar compound was also isolated (120mg, 25%) and corresponds to the bis-alkylated derivative (characterization not included). **^{1}H NMR (DMSO, 400 MHz):** δ (ppm): 2.03 (2H, m, 2H8'), 2.74 (2H, t, $J_{7'-8'}$= 7.6 Hz, 2H7'), 3.28 (2H, t, $J_{9'-8'}$= 7.6 Hz, 2H9'), 7.09 to 7.13 (2H, m, H5 & H6), 7.18 (1H, m, H4'), 7.22 (2H, m, H2' & H6'), 7.29 (2H, m, H3' & H5'), 7.44 (2H, bs, H4 & H7) **^{13}C NMR (DMSO, 100 MHz):** δ (ppm): 36.0 (C9'), 36.2 (C8'), 39.2 (C7'), 126.5 (bs, C5 & C6), 131.1 (C4'), 133.6 (C2', C3', C5' & C6'), 146.3 (C1'), 155.2 (C2) **MS:** ESI: m/z: 269.1 ($[M+H]^+$) **HRMS (ESI):** calculated for $C_{16}H_{17}N_2S$: m/z = 269.1107, found: 269.1120

2-[(3-phenoxypropyl)thio]-1*H*-benzimidazole (44): To a mixture of 1*H*-benzimidazole-2-thiol (200 mg, 1.33 mmol, 1.0 eq.), K_2CO_3 (370 mg, 2.66 mmol, 2.0 eq.) and TBAI (147 mg, 0.40 mmol, 0.3 eq.) in acetonitrile (6 mL) was added 3-phenoxypropyl bromide (630 µL, 3.99 mmol, 3.0 eq.). The reaction mixture was stirred at 35°C (oil bath at 40°C) during 48 h and then, diluted with water and extracted with methyl *tert*-butyl ether. The organic layer was dried over Na_2SO_4, the solvent removed under reduced pressure and the residue purified by silica gel flash-column chromatography (eluent: heptane/EtOAc, 90/10 to 70/30) to afford compound **44** (260 mg, 69 %) as a white solid. **^{1}H NMR (DMSO, 400 MHz):** δ (ppm): 2.19 (2H, q, $J_{9'-8'}$= $J_{9'-10'}$= 6.4 Hz, 2H9'), 3.42 (2H, t, $J_{10'-9'}$= 6.4 Hz, 2H10'), 4.10 (2H, t, $J_{8'-9'}$= 6.4 Hz, 2H8'), 6.91-6.96 (3H, m, H4', H2' & H6'), 7.12 (2H, m, H5 & H6), 7.28 (2H, m, H3' & H5'), 7.37 (1H, bs, H7),

7.51 (1H, bs, H4), 12.6 (1H, s, benzimidazolic H) **^{13}C NMR (DMSO, 100 MHz):** δ (ppm): 28.5 (C10'), 29.4 (C9'), 66.2 (C8'), 110.7 (C7), 114.9 (C2' & C6'), 117.8 (C4), 121.0 (C4'), 121.6 & 122.0 (C5 & C6), 130.0 (C4'), 129.9 (C3' & C5'), 150.3 (C2), 158.9 (C1') **MS:** ESI: m/z: 285.1 ($[M+H]^+$) **HRMS (ESI):** calculated for $C_{16}H_{17}N_2OS$: m/z = 285.1069, found: 285.1054

2-[(2-phenylethyl)thio]-1*H*-benzimidazole (45): To a mixture of 1*H*-benzimidazole-2-thiol (200 mg, 1.33 mmol, 1.0 eq.), K_2CO_3 (370 mg, 2.66 mmol, 2.0 eq.) and TBAI (295 mg, 0.80 mmol, 0.6 eq.) in acetonitrile (6 mL) was added (3-bromopropyl)benzene (606 µL, 3.99 mmol, 3.0 eq.). The reaction mixture was stirred at 35°C (oil bath at 40°C) during 48 h and then, diluted with water and extracted with ethyl acetate. The organic layer was dried over Na_2SO_4, evaporated under reduced pressure and the residue was purified by silica gel flash-column chromatography (eluent: heptane/EtOAc, 90/10 to 70/30) to afford compound **45** (260 mg, 77 %) as a white solid. *NB*: A less polar compound was also isolated (80 mg, 17 %, white solid) and corresponds to the *N,S*-bis-alkylated derivative (characterization not included). **^{1}H NMR (DMSO, 400 MHz):** δ (ppm): 3.73 (2H, t, $J_{9'-8'}$= 6.4 Hz, 2H9'), 4.36 (2H, t, $J_{8'-9'}$= 6.4 Hz, 2H8'), 6.94 (1H, m, H4'), 6.96 (2H, m, H2' & H6'), 7.28 (2H, tm, $J_{3'-2'}$= $J_{3'-4'}$= $J_{5'-6'}$= $J_{5'-4'}$= 7.4 Hz, H3' & H5'), 7.32-7.35 (2H, m, H5 & H6), 7.6-7.67 (2H, m, H4 & H7). **^{13}C NMR (DMSO, 100 MHz):** δ (ppm): 30.9 (C9'), 65.7 (C8'), 110.2 (C7), 114.5 (C2' & C6'), 118.2 (C4), 120.9 (C4'), 124.3 & 124.6 (C5 & C6), 129.5 (C3' & C5'), 141.2 (C3a), 151.3 (C2), 157.9 (C1'), 164.0 (C7a). **MS:** ESI: m/z: 272.1 ($[M+H]^+$) HRMS (ESI): calculated for $C_{15}H_{14}NO_2S$: m/z = 272.0740, found: 272.0750.

2{[2-(*o*-tolyloxy)ethyl]thio}-1*H*-benzimidazole (46): To a mixture of 1*H*-benzimidazole-2-thiol (0.50 g, 3.33 mmol, 1.0 eq.), K_2CO_3 (0.93 g, 6.66 mmol, 2.0 eq.) and TBAI (0.37 g, 1.00 mmol, 0.3 eq.) in acetonitrile (20 mL) was added 1-(2-bromoethoxy)-2-

methylbenzene (2.15 g, 9.99 mmol, 3.0 eq.). The reaction mixture was stirred at 35°C (oil bath at 40°C) during 16 hours and then diluted with water and extracted with ethyl acetate. The organic layer was dried over Na_2SO_4 and evaporated under reduced pressure. The residue was purified by silica gel flash-column chromatography (eluent: heptane/EtOAc, 90/10 to 70/30) to afford compound **46** (580 mg, 61 %) as a white solid. *NB*: A less polar compound was also isolated (300 mg, 22 %, pale oil) and corresponds to the *N,S*-bis-alkylated derivative (characterization not included). **^{1}H NMR (DMSO, 400 MHz):** δ (ppm): 2.11 (3H, s, methyl), 3.70 (2H, t, $J_{9'-8'}$= 6.4 Hz, 2H9'), 4.32 (2H, t, $J_{8'-9'}$= 6.4 Hz, 2H8'), 6.84 (1H, t, $J_{4'-3'}$= $J_{4'-5'}$= 7.8 Hz, H4'), 7.01 (1H, d, $J_{3'-4'}$= $J_{5'-4'}$= 7.8 Hz, H3'), 7.10 to 7.16 (4H, m, H5, H6, H5' & H6'), 7.38 (1H, bs, H4), 7.51 (1H, bs, H7). **^{13}C NMR (DMSO, 100 MHz):** δ (ppm): 16.3 (methyl), 31.0 (C9'), 67.1 (C8'), 110.6 (C7), 112.0 (C3'), 117.7 (C4), 121.0 (C4'), 121.8 (bs, C5 & C6), 126.3 (C2'), 127.5 (C3'), 130.9 (C5'), 150.3 (C2), 156.6 (C1'). **MS:** ESI: m/z: 285.1 ($[M+H]^+$) HRMS (ESI): calculated for $C_{16}H_{17}N_2OS$: m/z = 285.1056, found: 285.1034.

2-{[2-(*p*-tolyloxy)ethyl]thio}-1*H*-benzimidazole (48): To a mixture of 1*H*-benzimidazole-2-thiol (200 mg, 1.33 mmol, 1.0 eq.), K_2CO_3 (370 mg, 2.66 mmol, 2.0 eq.) and TBAI (147 mg, 0.40 mmol, 0.3 eq.) in acetonitrile (12 mL) was added (2-bromoethoxy)-4-methylbenzene (860 mg, 3.99 mmol, 3.0 eq.). The reaction mixture was stirred at 35°C (oil bath at 40°C) during 20 h and then filtered and evaporated under reduced pressure. The residue was purified by silica gel flash-column chromatography (eluent: heptane/EtOAc, 90/10 to 70/30) to afford compound **48** (130 mg, 34 %) as white solid. Note : Another compound was also isolated (300 mg, 54 %) %) and corresponds to the bis-alkylated derivative (characterization not included). **^{1}H NMR (DMSO, 400 MHz):** δ (ppm): 2.22 (3H, s, methyl), 3.65 (2H, t, $J_{9'-8'}$= 6.4 Hz, 2H9'), 4.27 (2H, t, $J_{8'-9'}$= 6.4 Hz, 2H8'), 6.88 (2H, dm, $J_{2'-3'}$= $J_{6'-5'}$= 8.2 Hz, H2' & H6'),

7.08 (2H, d, $J_{3'-2'}$= $J_{5'-6'}$= 8.6 Hz, H3' & H5'), 7.12 (2H, m, H5 & H6), 7.45 (2H, bs, H4 & H7) **^{13}C NMR (DMSO, 100 MHz):** δ (ppm): 20.5 (methyl), 30.7 (C9'), 66.9 (C8'), 114.9 (C2' & C6'), 121.8 (C5 & C6), 130.0 (C4'), 130.3 (C3' & C5'), 150.2 (C2), 156.5 (C1') **MS:** ESI: m/z: 285.1 ($[M+H]^+$) **HRMS (ESI):** calculated for $C_{16}H_{17}N_2OS$: m/z = 285.1056, found: 285.1054

2{[2-(2,6-dimethylphenoxy)ethyl]thio}-1*H*-benzimidazole (49): To a mixture of 1*H*-benzimidazole-2-thiol (0.50 g, 3.33 mmol, 1.0 eq.), K_2CO_3 (0.93 g, 6.66 mmol, 2.0 eq.) and TBAI (0.37 g, 1.00 mmol, 0.3 eq.) in acetonitrile (20 mL) was added 2-(2-bromoethoxy)-1,3-dimethylbenzene (2.29 g, 9.99 mmol, 3.0 eq.). The reaction mixture was stirred at 35°C (oil bath at 40°C) during 16 h and then diluted with water and extracted with ethyl acetate. The organic layer was dried over Na_2SO_4 and evaporated under reduced pressure. The residue was purified by silica gel flash-column chromatography (eluent: heptane/EtOAc, 90/10 to 70/30) to afford compound **49** (450 mg, 45 %) as a white solid. Note: A less polar compound was also isolated (350 mg, 24 %, orange oil) and corresponds to the *N,S*-bis-alkylated derivative (characterization not included). **^{1}H NMR (DMSO, 400 MHz):** δ (ppm): 2.24 (6H, s, methyl), 3.70 (2H, t, $J_{9'-8'}$= 6.4 Hz, 2H9'), 4.08 (2H, t, $J_{8'-9'}$= 6.4 Hz, 2H8'), 6.91 (1H, t, $J_{4'-3'}$= $J_{4'-5'}$= 7.8 Hz, H4'), 7.01 (2H, d, $J_{3'-4'}$= $J_{5'-4'}$= 7.8 Hz, H3' & H5'), 7.10 to 7.14 (2H, m, H5 & H6), 7.37 (1H, bs, H4), 7.50 (1H, bs, H7) **^{13}C NMR (DMSO, 100 MHz):** δ (ppm): 16.5 (2 methyl), 31.8 (C9'), 70.7 (C8'), 110.8 (C7), 117.7 (C4), 121.6 & 122.1 (C5 & C6), 124.3 (C4'), 129.2 (C3' & C5'), 130.8 (C2' & C6'), 136.0 (C7a), 144.1 (C3a), 150.4 (C2), 155.5 (C1') **MS:** ESI: m/z: 299.1 ($[M+H]^+$) **HRMS (ESI):** calculated for $C_{17}H_{19}N_2OS$: m/z = 299.1213, found: 299.1190

2-[(2-phenoxyethyl)thio]-1*H*-indole (53): To a mixture of indoline-2-thione (0.60 g, 4.0 mmol, 1.0 eq.), K_2CO_3 (1.1 g, 8.0 mmol, 2.0 eq.) and TBAI (0.9 g, 2.4 mmol, 0.6 eq.) in acetonitrile (30 mL) was added (2-bromoethoxy)benzene (1.6 g, 8.0 mmol, 2.0 eq.). The reaction

mixture was stirred at room temperature during 12 h then, diluted with water and extracted with ethyl acetate. The organic layer was dried over Na_2SO_4, evaporated under reduced pressure, and the residue was purified by silica gel flash-column chromatography (eluent: heptane/EtOAc, 95/5 to 85/15) to afford compound **53** (0.7 g, 65 %) as a white solid. **^{1}H NMR (DMSO, 400 MHz):** δ (ppm): 3.29 (2H, t, $J_{9'-8'}$= 6.4 Hz, 2H9'), 4.15 (2H, t, $J_{8'-9'}$= 6.4 Hz, 2H8'), 6.57 (1H, bs, H3), 6.90 (2H, dm, $J_{2'-3'}$= $J_{6'-5'}$= 7.4 Hz, H2' & H6'), 6.93 (1H, tm, $J_{4'-3'}$= $J_{4'-5'}$= 7.4 Hz, H4'), 6.99 (1H, tm, J_{6-5}= J_{6-7}= 7.8 Hz, H6), 7.09 (1H, tm, J_{5-4}= J_{5-6}= 7.8 Hz, H5), 7.26 (2H, tm, $J_{3'-2'}$= $J_{3'-4'}$= $J_{5'-6'}$= $J_{5'-4'}$= 7.4 Hz, H3' & H5'), 7.32 (1H, d, J_{4-5}= 7.8 Hz, H4), 7.46 (1H, d, J_{7-6}= 7.8 Hz, H7), 11.44 (1H, s, indolic H) **^{13}C NMR (DMSO, 100 MHz):** δ (ppm): 34.4 (C9'), 66.7 (C8'), 106.8 (C3), 111.3 (C4), 114.9 (C2' & C6'), 119.7 (C6), 119.9 (C7), 121.3 (C4'), 122.1 (C5), 128.5 (C3a), 128.8 (C2), 130.0 (C3' & C5'), 137.9 (C7a), 158.6 (C1') **MS:** ESI: m/z: 270.1 ($[M+H]^+$) **HRMS (ESI):** calculated for $C_{16}H_{16}NOS$: m/z = 270.0947, found: 270.0956

Synthetic procedure for N-(2-phenoxyethyl)-1H-benzo[d]imidazol-2-amine (**38**), 2-(3-phenoxypropyl)-1H-benzo[d]imidazole (**39**), N-(2-((1H-benzo[d]imidazol-2-yl)thio)ethyl)aniline (**43**), 2-((2-(m-tolyloxy)ethyl)thio)-1H-benzo[d]imidazole (**47**), 2-((2-(3-chlorophenoxy)ethyl)thio)-1H-benzo[d]imidazole (**50**), 2-((2-(4-chlorophenoxy)ethyl)thio)-1H-benzo[d]imidazole (**51**) is mentioned in supporting information (Supporting Figure 19-20). These compounds were synthesized at Enamine (http://www.enamine.net/). 4-(2-((1H-benzo[d]imidazol-2-yl)thio)ethoxy) benzenesulfonamide (**52**), 2-((2-phenoxyethyl)thio)-1H-indole-7-sulfonamide (**54**) were obtained from Enamine's stock.

Preparation of the Protein Structure for Docking: AR crystal structure complexed with compound **1**, 2YLO (2.50Å resolution)[19] and 4HLW (2.50Å resolution) were used for molecular docking studies. For protein structure preparation, all solvent molecules have been

deleted and the bond order for the ligand and protein has been adjusted. The missing hydrogen atoms have been added, and side chains have then been energy-minimized using the OPLS-2005 force field, as implemented by Maestro.[29] The ligand binding region has been defined by a 12Å box centered on the crystallographic ligands of the crystal structures. No Van der Waals scaling factors were applied; the default settings were used for all other adjustable parameters.

Ligand Preparation: All the compounds were built using MOE version 2009.[30]Hydrogen atoms were added after these structures were "washed" (a procedure including salt disconnection, removal of minor components, deprotonation of strong acids, and protonation of strong bases). The following energy minimization was performed with the MMFF94x force field, as implemented by the MOE, and the optimized structures were exported into the Maestro suite in SD file format.

Molecular docking: Docking experiments were performed using Glide[31] included in Schrodinger Package, Maestro interface version 9.0.[29] For docking, standard-precision (SP) docking method was adopted to generate the minimized pose, and the Glide scoring function (Glide Score) was used to select the final poses for each ligand.

Heterologous Expression of the AR: The AR ligand binding domain (LBD) was expressed and purified as previously described. [16]

eGFP Cellular AR Transcription Assay: AR transcriptional activity was assayed as previously described.[22] Briefly, stably transfected eGFP-expressing LNCaP human prostate cancer cells (LN-ARR2PBeGFP) containing an androgen-responsive probasin-derived promoter (ARR2PB) were grown in phenol-red-free RPMI 1640 supplemented with 5% CSS for 5 days. The cells were then seeded into a 96-well plate (35,000cells/well) and treated the next day with

0.1nM R1881 and increasing concentrations (0-100μM) of compound. After 3 days of treatment the fluorescence was measured (excitation, 485 nm; emission, 535 nm).

Prostate Surface Antigen assay: The evaluation of PSA excreted into the media was performed in parallel to the eGFP assay using the same plates (see above description). After the cells were incubated for 3 days 150μl of the media was taken from each well, and added to 150μl of PBS. PSA levels were then evaluated using Cobas e 411 analyzer instrument (Roche Diagnostics) according to the manufacturer's instructions.

MTS Assay: Cell proliferation was determined using the MTS cell proliferation assay following incubation with the compound (0-100μM) over 72h (CellTiter 961 Aqueous One Solution Reagent, Promega). In brief, 30μL of the reagent was added to cells in each well of the 96-well plate containing 200μL of media and incubated for 90 minutes at 37°C in 5% CO_2. The production of formazan was measured at 490 nm.

Luciferase ER-α transcriptional assay: ER-α positive MCF-7 human breast cancer cells were grown in phenol-red-free RPMI 1640 supplemented with 10% CSS for 5 days. The cells were seeded on a 96-well plate (30,000cells/well). After 24 hours, the cells were transfected with 50 ng luciferase plasmid using Lipofectamine 2000 reagent (Invitrogen) and treated the next day with either the test compounds or Tamoxifen in the presence of 1 nM E2. The final concentration of the compounds was 10 μM and Tamoxifen was added at 3 different concentrations, 10 μM, 5 μM and 1 μM. The medium contained 0.1% (v/v) EtOH and 0.1 % (v/v) DMSO. 24 hours after treatment the medium was aspirated off and the cells were lysed by adding 65 μL of 1X passive lysis buffer (Promega). The plates were placed on a shaker at room temperature for 15 mins and then subjected to two freeze thaw cycles to help lyse the cells. 20 μL of the lysate from each treatment was transferred onto a 96 well white flat bottom plate

(Corning) and the luminescence signal was measured after adding 50 µL of the luciferase assay reagent (Promega).

Bio-Layer Interferometry (BLI) assay: The direct reversible interaction between small molecules and the AR was quantified by BLI using OctetRED (ForteBio). The LDB of the biotinylated androgen receptor (bAR) was produced in situ with AviTag technology.[32] The AviTag sequence (GLNDIFEAQKIEWHE) followed by a six residue glycine serine linker (GSGSGS) was incorporated at the N-terminus of the AR LBD (669-919). Escherichia coli BL21 containing both biotin ligase and AR LBD vectors were induced with 0.5mMisopropyl-β-D-thiogalactopyranoside (IPTG) in the presence of dihydrotestosterone (DHT) and biotin at 16°C overnight. The bacteria were then lysed by sonication, and the resulting lysate was purified by immobilized metal ion affinity chromatography (IMAC) with nickel_nitrilotriacetic acid (Ni_NTA) resin and cation-exchange chromatography (HiTrap SP).

Purified bAR LBD (50µg/mL) was bound to the super-streptavidin sensors overnight at room temperature. The sensor was kept in assay buffer [150 mM Lithium Sulfate, 50 mM HEPES, 1 mM DTT and 10 µM DHT]. In all experiments, a known AF2-interacting peptide was used as a control to confirm functionality of the bAR LBD.

Androgen Displacement Assay: Androgen displacement was assessed with the Polar Screen Androgen Receptor Competitor Green Assay Kit as per the instructions of the manufacturer.

Peptide Displacement Assay: Peptide displacement was assessed as described in our previous work. [12, 19]

Determination of Compound Purity: Compound identity and purity were confirmed by LC_MS/MS. Briefly, an Acquity ultraperformance liquid chromatograph (UPLC) with a 2.1*

100 mm BEH, 1.7μM, C18 column coupled to a photodiode array (PDA) detector in line with a Quattro Premier XE (Waters, Milford, MA) was used with water and acetonitrile containing 0.1% formic acid as mobile phases. A 5-95% acetonitrile gradient from 0.2-10.0 min was used, and 95% was maintained for 2 min followed by re-equilibration to starting conditions for a total run time of 15.0 min. The MS was run at unit resolution with 3 kV capillary, 120 and 300°C source and desolvation temperatures, 50 and 1000 L/h cone and desolvation N2 gas flows, and Ar collision gas set to 7.4-3 mbar. On the basis of the full range of the diode array absorbance (210-800 nm), the relative purity [AUCCMPD versus area under the curve (AUC) of all other peaks] was calculated. All compounds described had a purity of >90-95%.

Protein Expression, Purification, Crystallization and Data Collection: The LBD of human AR containing amino acid residues 663-919 was expressed as a glutathione S-transferase fusion protein in E. coli BL21 (DE3) cells, which were grown in 2-YT medium at 18°C. Testosterone (200μM) was added into cell culture medium before induction with 100mM IPTG. The fusion protein was purified by glutathione-sepharose affinity chromatography and, subsequently, cleaved with thrombin. The protein was further purified by cation-exchange chromatography. To stabilize the LBD of the AR, all solutions used for purification contained 50μM testosterone.

The binary complex of AR LBD and testosterone was crystallized using the sitting drop vapor-diffusion method at 294K. The protein sample contained 3 mg/mL AR LBD, 50μM testosterone, 50mM NaCl, 70mM Li_2SO_4, 0.1%n-octyl-β-glucoside, and 40mMTris-HCl at pH 7.5. The well solution contained 0.35MNa_2HPO_4/K_2HPO_4, 0.1M $(NH_4)_2HPO_4$, 7.0% polyethylene glycol 400 (PEG 400), and 50mM Tris-HCl at pH 7.5. Crystals were selected and then soaked in 8.0mM compound **32.**

Single crystals were flash-frozen in liquid nitrogen after soaking with the compound for 16h. X-ray diffraction data sets were collected using beamline 5.0.3 at the Lawrence Berkeley National Laboratory Advanced Light Source. Data sets were processed with iMosflm. The best data set collected had 98% completeness at 2.2Å resolution. The crystal space group is $P2_12_12_1$, with unit cell parameters of a = 55.9, b = 66.2, and c = 72.9Å.

Structure Solution and Refinement: The ternary complex structure was solved by molecular replacement using Phaser.[33] The coordinate of the AR LBD-testosterone complex (PDB code 2AM9) was used as the search model, however, with testosterone removed. The structure was refined to 2.5Å resolution using Phenix[34] and Refmac.[35] The extra density of testosterone was clearly observed at the initial refinement step. A characteristic electron density of the compound was observed at the BF3 binding site.

Compound **32** was fit according to the electron density map using the COOT program. [36] Because the compound binding is quite flexible, its occupancy was set as 0.5 during the refinement. The free R factor and R factors of the final mode of the ternary complex are 1.88 and 2.50, respectively, with good stereochemistry (Table 2). All crystallographic experiments have been carried out as contract research by Structure-Based Design, Inc. (www.strbd.com).

AKCNOWLEDGMENTS

This work was supported by a Proof-of Principle CIHR grant and the PC-STAR Project, which is funded by Prostate Cancer Canada with the support of Safeway. The authors thank Jeffrey Leong for helping *in vitro* experiments, Dr. Vladimir Ivanov for providing synthetic analogues, Dr. Maia Vinogradova for her assistance with crystallographic experiments and Hong Zheng and Eleanore Hendrickson of the Structure-Based Design for their valuable contributions. The determination of the structures of the BF3 binder with the AR has been done by the *Structure-Based Design* Company (www. strbd.com) as a contract research. The authors are also grateful to the staff at the Lawrence Berkeley National Laboratory for assistance with X-ray data collection, and we thank Hans Adomat for his considerable assistance conducting the LC/MS analysis. The authors thank Drs. Martin Gleave, Amina Zoubeidi for providing us with Enzalutamide-resistant LNCaP cells. The authors (RNY and CL) acknowledge the support of the British Columbia Government Leading Edge Endowment Fund.

REFERENCES

1. Roy, A. K.; Lavrovsky, Y.; Song, C. S.; Chen, S.; Jung, M. H.; Velu, N. K.; Bi, B. Y.; Chatterjee, B. Regulation of androgen action. *Vitam Horm* **1999**, *55*, 309-352.

2. Taplin, M. E.; Rajeshkumar, B.; Halabi, S.; Werner, C. P.; Woda, B. A.; Picus, J.; Stadler, W.; Hayes, D. F.; Kantoff, P. W.; Vogelzang, N. J.; Small, E. J. Androgen receptor mutations in androgen-in dependent prostate cancer: Cancer and Leukemia Group B Study 9663. *J.Clin. Oncol.* **2003,** *21*, 2673-2678.

3. Tilley, W. D.; Limtio, S. S.; Horsfall, D. J.; Aspinall, J. O.; Marshall, V. R.; Skinner, J. M. Detection of Discrete Androgen Receptor Epitopes in Prostate-Cancer by Immunostaining-Measurement by Color Video Image-Analysis. *Cancer Res.* **1994,** *54*, 4096-4102.

4. Albertsen, P. C.; Hanley, J. A.; Fine, J. 20-year outcomes following conservative management of clinically localized prostate cancer. *JAMA-J. Am. Med. Assoc.* **2005,** *293*, 2095-2101.

5. Gleave, M.; Goldenberg, S. L.; Bruchovsky, N.; Rennie, P. Intermittent androgen suppression for prostate cancer: rationale and clinical experience. *Prostate Cancer and Prostatic Dis.* **1998,** *1*, 289-296.

6. Lassi, K.; Dawson, N. A. Emerging therapies in castrate-resistant prostate cancer. *Curr.Opin. Oncol.* **2009,** *21*, 260-265.

7. Tran, C.; Ouk, S.; Clegg, N. J.; Chen, Y.; Watson, P. A.; Arora, V.; Wongvipat, J.; Smith-Jones, P. M.; Yoo, D.; Kwon, A.; Wasielewska, T.; Welsbie, D.; Chen, C. D.; Higano, C. S.; Beer, T. M.; Hung, D. T.; Scher, H. I.; Jung, M. E.; Sawyers, C. L. Development of a Second-Generation Antiandrogen for Treatment of Advanced Prostate Cancer. *Science* **2009,** *324*, 787-790.

8. Clegg, N. J.; Wongvipat, J.; Joseph, J. D.; Tran, C.; Ouk, S.; Dilhas, A.; Chen, Y.; Grillot, K.; Bischoff, E. D.; Cal, L.; Aparicio, A.; Dorow, S.; Arora, V.; Shao, G.; Qian, J.; Zhao, H.; Yang, G. B.; Cao, C. Y.; Sensintaffar, J.; Wasielewska, T.; Herbert, M. R.; Bonnefous, C.; Darimont, B.; Scher, H. I.; Smith-Jones, P.; Klang, M.; Smith, N. D.; De Stanchina, E.; Wu, N.; Ouerfelli, O.; Rix, P. J.; Heyman, R. A.; Jung, M. E.; Sawyers, C. L.; Hager, J. H. ARN-509: A Novel Antiandrogen for Prostate Cancer Treatment. *Cancer Res.* **2012,** *72*, 1494-1503.

9. Furr, B. J. A. The Development of Casodex(TM) (bicalutamide): Preclinical studies. *Eur.Urol.* **1996,** *29*, 83-95.

10. Chen, Y.; Clegg, N. J.; Scher, H. I. Anti-androgens and androgen-depleting therapies in prostate cancer: new agents for an established target. *Lancet Oncol.* **2009,** *10*, 981-991.

11. Gao, W. Q.; Bohl, C. E.; Dalton, J. T. Chemistry and structural biology of androgen receptor. *Chem. Rev.* **2005,** *105*, 3352-3370.

12. Axerio-Cilies, P.; Lack, N. A.; Nayana, M. R. S.; Chan, K. H.; Yeung, A.; Leblanc, E.; Guns, E. S. T.; Rennie, P. S.; Cherkasov, A. Inhibitors of Androgen Receptor Activation Function-2 (AF2) Site Identified through Virtual Screening. *J.Med. Chem.* **2011,** *54*, 6197-6205.

13. Caboni, L.; Kinsella, G. K.; Blanco, F.; Fayne, D.; Jagoe, W. N.; Carr, M.; Williams, D. C.; Meegan, M. J.; Lloyd, D. G. "True" Antiandrogens-Selective Non-Ligand-Binding Pocket Disruptors of Androgen Receptor-Coactivator Interactions: Novel Tools for Prostate Cancer. *J.Med. Chem.* **2012,** *55*, 1635-1644.

14. Feau, C.; Arnold, L. A.; Kosinski, A.; Zhu, F. Y.; Connelly, M.; Guy, R. K. Novel Flufenamic Acid Analogues as Inhibitors of Androgen Receptor Mediated Transcription. *ACS Chem. Biol.* **2009,** 4, 834-843.

15. Gunther, J. R.; Parent, A. A.; Katzenellenbogen, J. A. Alternative Inhibition of Androgen Receptor Signaling: Peptidomimetic Pyrimidines As Direct Androgen Receptor/Coactivator Disruptors. *ACS Chem. Biol.* **2009,** *4*, 435-440.

16. Estebanez-Perpina, E.; Arnold, A. A.; Nguyen, P.; Rodrigues, E. D.; Mar, E.; Bateman, R.; Pallai, P.; Shokat, K. M.; Baxter, J. D.; Guy, R. K.; Webb, P.; Fletterick, R. J. A surface on the androgen receptor that allosterically regulates coactivator binding. *P.Natl. Acad. Sci. U.S.A.* **2007**, *104*, 16074-16079.

17. De Leon, J. T.; Iwai, A.; Feau, C.; Garcia, Y.; Balsiger, H. A.; Storer, C. L.; Suro, R. M.; Garza, K. M.; Lee, S.; Kim, Y. S.; Chen, Y.; Ning, Y. M.; Riggs, D. L.; Fletterick, R. J.; Guy, R. K.; Trepel, J. B.; Neckers, L. M.; Cox, M. B. Targeting the regulation of androgen receptor signaling by the heat shock protein 90 cochaperone FKBP52 in prostate cancer cells. *P.Natl. Acad. Sci. U.S.A.* **2011,** *108*, 11878-11883.

18. Grosdidier, S.; Carbo, L. R.; Buzon, V.; Brooke, G.; Nguyen, P.; Baxter, J. D.; Bevan, C.; Webb, P.; Estebanez-Perpina, E.; Fernandez-Recio, J. Allosteric Conversation in the Androgen Receptor Ligand-Binding Domain Surfaces. *Mol. Endocrinol.* **2012,** *26*, 1078-1090.

19. Lack, N. A.; Axerio-Cilies, P.; Tavassoli, P.; Han, F. Q.; Chan, K. H.; Feau, C.; LeBlanc, E.; Guns, E. T.; Guy, R. K.; Rennie, P. S.; Cherkasov, A. Targeting the Binding Function 3 (BF3) Site of the Human Androgen Receptor through Virtual Screening. *J. Med. Chem.* **2011,** *54*, 8563-8573.

20. Instant JChem 5.10, ChemAxon. http://www.chemaxon.com

21. Irwin, J. J.; Sterling, T.; Mysinger, M. M.; Bolstad, E. S.; Coleman, R. G. ZINC: A Free Tool to Discover Chemistry for Biology. *J. Chem. Inf. Model.* **2012,** *52*, 1757-1768.

22. Tavassoli, P.; Snoek, R.; Ray, M.; Rao, L. G.; Rennie, P. S. Rapid, non-destructive, cell-based screening assays for agents that modulate growth, death, and androgen receptor activation in prostate cancer cells. *Prostate* **2007,** *67*, 416-426.

23. Balk, S. P.; Ko, Y. J.; Bubley, G. J. Biology of prostate-specific antigen. *J. Clin. Oncol.* **2003,** *21*, 383-391.

24. Horoszewicz, J. S.; Leong, S. S.; Chu, T. M.; Wajsman, Z. L.; Friedman, M.; Papsidero, L.; Kim, U.; Chai, L. S.; Kakati, S.; Arya, S. K.; Sandberg, A. A. The LNCaP cell line--a new model for studies on human prostatic carcinoma. *Prog. Clin. Biol. Res.* **1980,** *37*, 115-32.

25. Arkin, M. R.; Wells, J. A. Small-molecule inhibitors of protein-protein interactions: Progressing towards the dream. *Nat. Rev. Drug Discov.* **2004,** *3*, 301-317.

26. Arkin, M. R.; Randal, M.; DeLano, W. L.; Hyde, J.; Luong, T. N.; Oslob, J. D.; Raphael, D. R.; Taylor, L.; Wang, J.; McDowell, R. S.; Wells, J. A.; Braisted, A. C. Binding of small molecules to an adaptive protein-protein interface. *P.Natl. Acad. Sci. U.S.A.* **2003,** *100*, 1603-1608.

27. Szakacs, G.; Paterson, J. K.; Ludwig, J. A.; Booth-Genthe, C.; Gottesman, M. M. Targeting multidrug resistance in cancer. *Nat. Rev. Drug Discov.* **2006,** *5*, 219-234.

28. Seruga, B.; Ocana, A.; Tannock, I. F. Drug resistance in metastatic castration-resistant prostate cancer. *Nat. Rev. Clin. Oncol.* **2011,** *8*, 12-23.

29. Schrodinger. Maestro; Schrodinger: New York, 2008;. www. schrodinger.com.

30. Chemical Computing Group, Inc. (CCG). Molecular Operating Environment (MOE); CCG: Montreal, Quebec, Canada, 2008; . www. chemcomp.com.

31. Friesner, R. A.; Banks, J. L.; Murphy, R. B.; Halgren, T. A.; Klicic, J. J.; Mainz, D. T.; Repasky, M. P.; Knoll, E. H.; Shelley, M.; Perry, J. K.; Shaw, D. E.; Francis, P.; Shenkin, P. S.

Glide: A new approach for rapid, accurate docking and scoring. 1. Method and assessment of docking accuracy. *J.Med.Chem.* **2004,** *47*, 1739-1749.

32. Tirat, A.; Freuler, F.; Stettler, T.; Mayr, L. M.; Leder, L. Evaluation of two novel tag-based labelling technologies for site-specific modification of proteins. *Int.J. Biol. Macromol.* **2006,** *39*, 66-76.

33. McCoy, A. J.; Grosse-Kunstleve, R. W.; Adams, P. D.; Winn, M. D.; Storoni, L. C.; Read, R. J. Phaser crystallographic software. *J. Appl.Cryst.* **2007,** *40*, 658-674.

34. Adams, P. D.; Afonine, P. V.; Bunkoczi, G.; Chen, V. B.; Davis, I. W.; Echols, N.; Headd, J. J.; Hung, L.-W.; Kapral, G. J.; Grosse-Kunstleve, R. W.; McCoy, A. J.; Moriarty, N. W.; Oeffner, R.; Read, R. J.; Richardson, D. C.; Richardson, J. S.; Terwilliger, T. C.; Zwart, P. H. PHENIX: a comprehensive Python-based system for macromolecular structure solution. *Acta Cryst. D.* **2010,** *66*, 213-221.

35. Murshudov, G. N.; Vagin, A. A.; Dodson, E. J. Refinement of macromolecular structures by the maximum-likelihood method. *Acta Cryst. D.* **1997,** *53*, 240-255.

36. Emsley, P.; Lohkamp, B.; Scott, W. G.; Cowtan, K. Features and development of Coot. *Acta Cryst. D.* **2010,** *66*, 486-501.

FIGURES AND TABLES

Table1. *Structures and Measured Activities of the Analogues (2-31) of Compound* ***1*** *Retrieved by 2D Similarity Search and Proposed Synthetic Derivatives (32-37)*

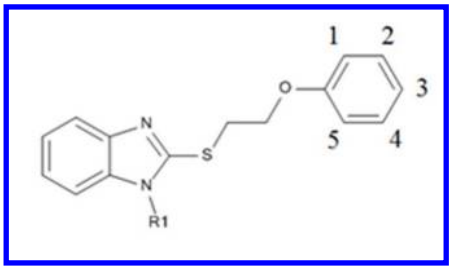

ID	AR transcriptional IC_{50} (μM)	R_1	1	2	3	4	5
2	11.1	CH_2-C(O)O-iPr	H	H	CH_3	H	H
3	12.7	C_2H_4OMe	H	H	CH_3	H	H
4	13.7	CH_2-C(O)O-iPr	H	H	H	CH_3	H
5	14.1	CH_2-C(O)OEt	H	CH_3	H	H	H
6	22.8	C_2H_4O-Ph(4-Me)	H	H	H	OC_2H_5	H
7	24.1	C_2H_4OMe	H	H	H	CH_3	H
8	30.6	CH_2-C(O)O-iPr	H	H	CH_3	CH_3	H
9	32.9	CH_2-C(O)OMe	H	H	CH_3	H	H
10	35	Et	H	H	H	CH_3	H
11	40.3	CH_2-C(O)OEt	H	H	CH_3	CH_3	H
12	45	Me	H	H	H	CH_3	H
13	55	CH_2C(O)OEt	H	H	H	C_2H_5	H
14	163.8	CH_2-C(O)O-	H	H	CH_3	H	H
15	>200	CH_2C(O)-N-Morph	H	H	H	CH_3	H
16	>200	CH_2-C(O)OMe	H	H	H	C_2H_5	H

17	>200	CH_2-C(O)OMe	H	H	CH_3	CH_3	H
18	>200	CH_2-C(O)OEt	H	CH_3	H	CH_3	H
19	>200	CH_2-C(O)O-	H	H	H	C_2H_5	H
20	>200	C_2H_4-C(O)O-	H	H	CH_3	H	H
21	>200	C_2H_4O-Ph	H	H	H	CH_3	H
22	>200	CH_2-C(O)O-	H	H	CH_3	CH_3	H
23	>200	CH_2-C(O)O-	H	H	H	CH_3	H
24	>200	C_2H_4-C(O)O-	H	CH_3	H	H	H
25	>200	C_2H_4-C(O)O-	H	H	H	CH_3	H
26	>200	$CH_2C(O)NEt_2$	H	H	H	CH_3	H
27	>200	CH_2-C(O)O-	H	CH_3	H	CH_3	H
28	>200	CH_2-C(O)O-	H	CH_3	H	H	CH_3
29	>200	CH_2-C(O)O-	H	H	H	t-Bu	H
30	>200	CH_2-C(O)O-Me	H	$CH_2CH{=}CH_2$	H	H	H
31	>200	C_2H_4-C(O)O-	H	H	H	C_2H_5	H
Synthetic Derivatives							
32	4.2	H	H	H	H	H	H
33	12	Et	H	H	H	H	H
34	>200	C_2H_4OH	H	H	H	H	H
35	>200	C_2H_4COOH	H	H	H	H	H
36	>200	$CH_2CH{=}CH_2$	H	H	H	H	H
37	>200	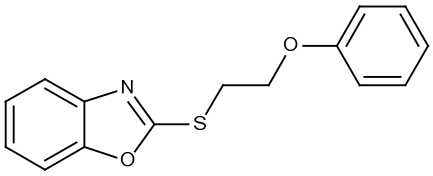					

Table2. *Data Collection and Refinement Statistics*

PDB Code	4HLW
X-ray Source	Synchrotron
Space Group	P212121
a, *b*, *c* (Å)	55.19, 66.30 and 73.01
α, β, γ (°)	90.0, 90.0 and 90.0
Data collection statistics	
Resolution (Å)	2.5
R_{sym} or R_{merge}	0.136/(0.580)
No. of unique reflections	12422/(1786)
I/σ (*I*)	7.01/(2.37)
Completeness (%)	99.93/(100)
Multiplicity	6.0/(6.2)
Refinement and model statistics	
Resolution (Å)	2.5
No. reflections used (work + test)	9717
$R_{work}{}^{a}$	0.188
$R_{free}{}^{a}$	0.250
No. of residues	244
No. of water molecules	13
Additional molecules	4
Total No. of atoms	1953
R.M.S.D bond length (Å)	0.029
R.M.S.D bond angles (Å)	1.21
Wilson B-factor (Å^2)	35.4
Mean B-factor (Å^2)	47
Ramachandran statistics (%)	
Favored region	98.0

Additional allowed region	7.0
Generously allowed region	0.9
Disallowed	0

[a] R_{work} and $R_{free} = \Sigma_h||Fo(h) - F_c(h)||/\Sigma_h||$ for the working set and test set (5%) of reflections, where $Fo(h)$ and $Fc(h)$ are the observed and calculated structure factor amplitudes for reflection.

Table3. *Structures and Measured Activities of the Synthetic Derivatives of Compound 32 with Different Linkers Attached.*

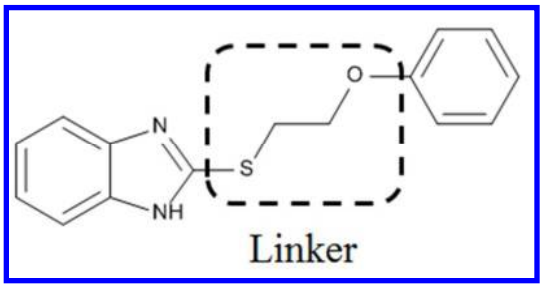

ID	AR transcriptional IC_{50} (μM)	Linker
38	>200	
39	>200	
40	>200	
41	>200	
42	12	
43	>200	
44	>200	

45	7.4	

Table4. *Structure and Activity Data for Synthetic Derivatives with Different Substitutions around Phenyl Ring*

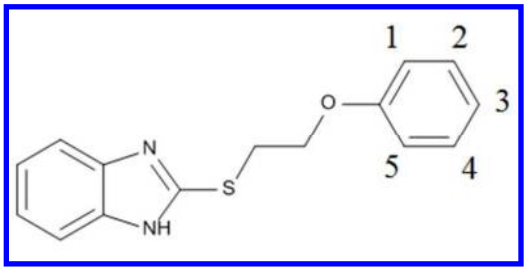

ID	AR transcriptional IC_{50} (μM)	1	2	3	4	5
46	19	CH_3	H	H	H	H
47	1.8	H	CH_3	H	H	H
48	7	H	H	CH_3	H	H
49	2.7	CH_3	H	H	H	CH_3
50	5	H	Cl	H	H	H
51	4	H	H	Cl	H	H
52	62	H	H	SO_2NH_2	H	H

***Table5**. Structure and Activity Data for 2-((2-phenoxyethyl) thio)-1H-indoles*

ID	AR transcriptional IC_{50} (μM)	Structure
53	5.4	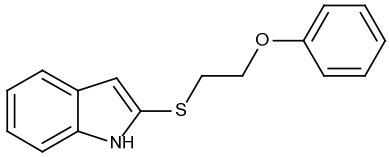
54	1.5	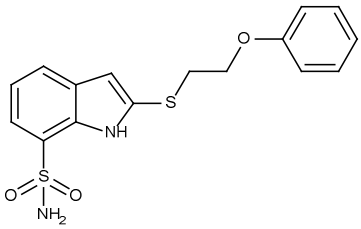

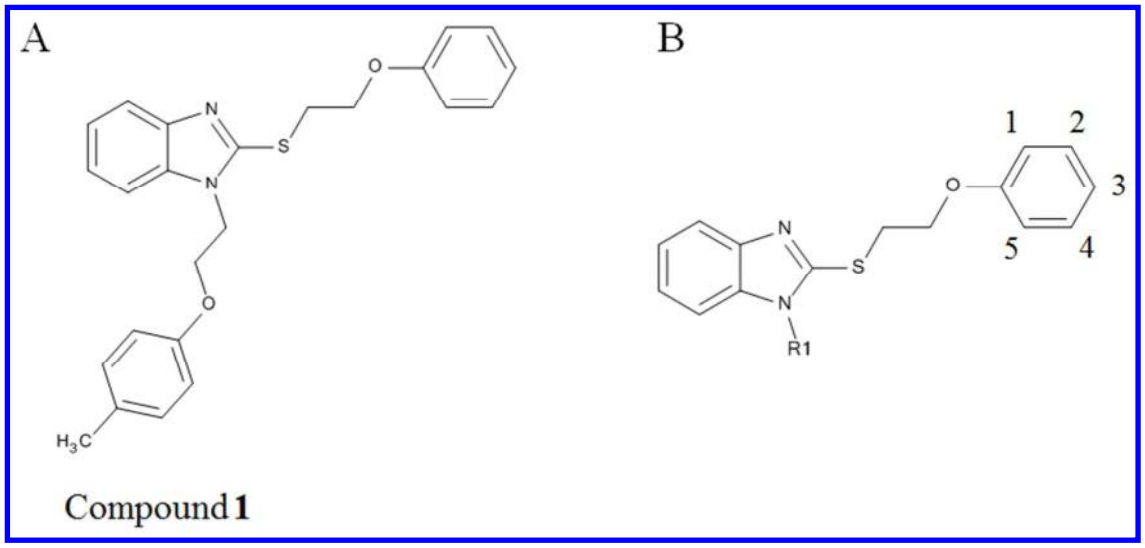

Figure 1. *A) Previously identified AR BF3 inhibitor B) Chemical template used as a query to find analogues of compound* ***1*** *by 2D similarity search method.*

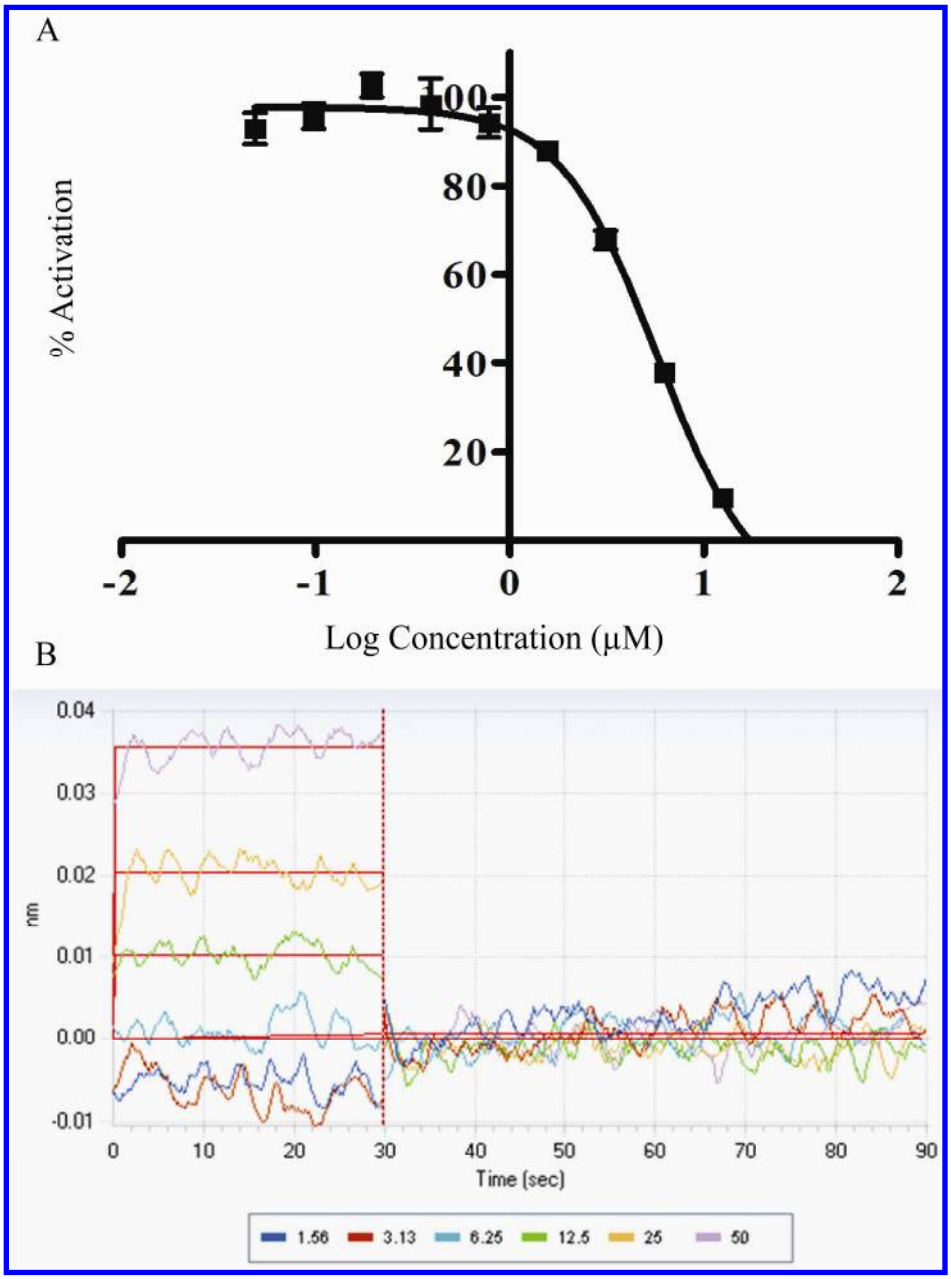

Figure 2. *A) Dose-response curve (0-25μM) illustrating the inhibiting effect of the compound* ***32*** *on the AR transcriptional activity in cells. Data points represent the mean of two independent experiments performed in triplicate. Error bars represent the standard error of the mean (SEM) for n = 6 values. Data was fitted using log of concentration of the inhibitors vs % activation with GraphPad Prism 6. B) BLI dose-response curves (0-50μM) reflecting the direct binding of the compound* ***32****.*

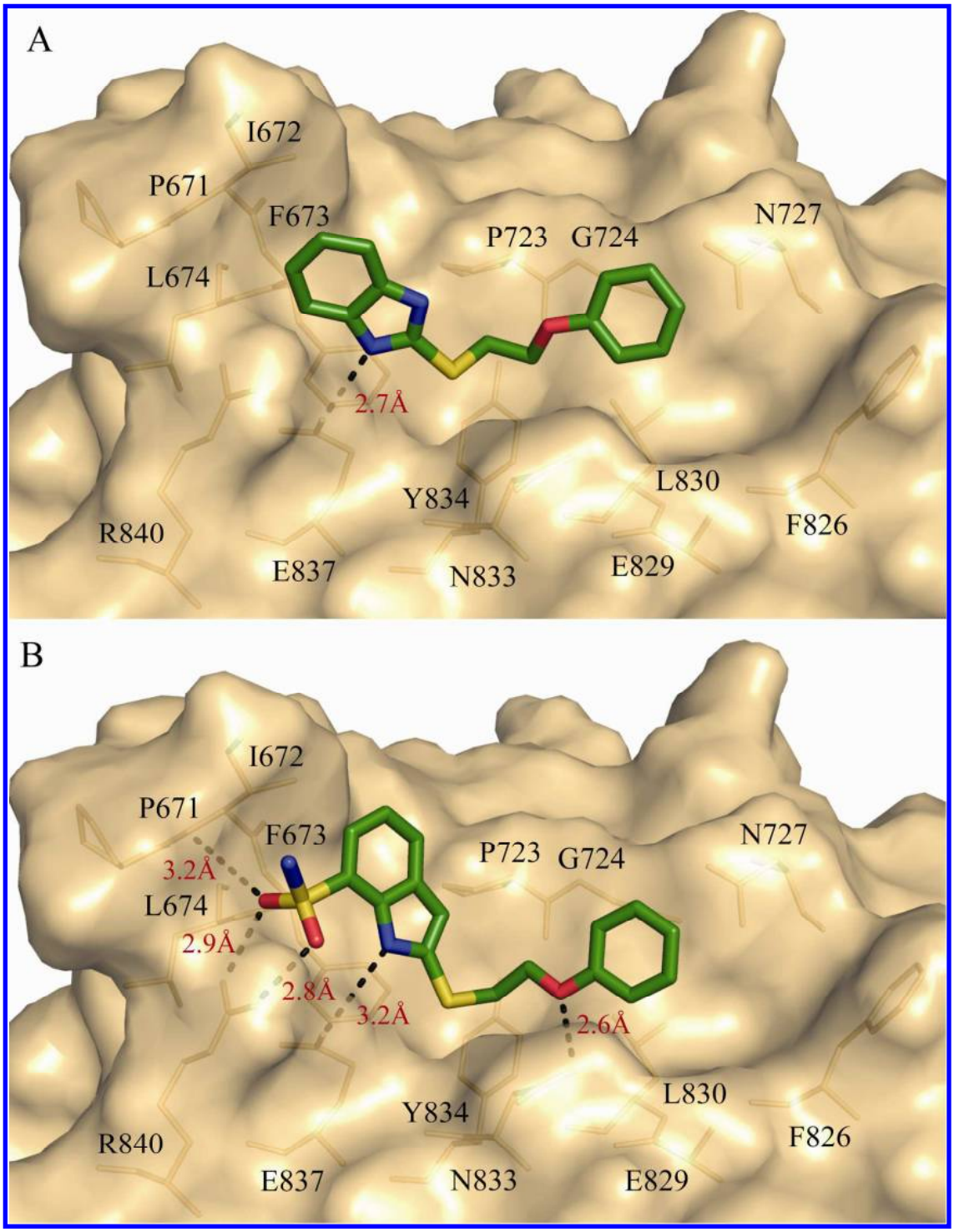

Figure 3. *A) X-ray crystal structure of compound* ***32*** *bound to BF3 pocket on the surface of human AR. Hydrogen bonds are shown in red. B) Binding orientation of compound* ***54*** *inside the BF3. Hydrogen bonds are shown in black.*

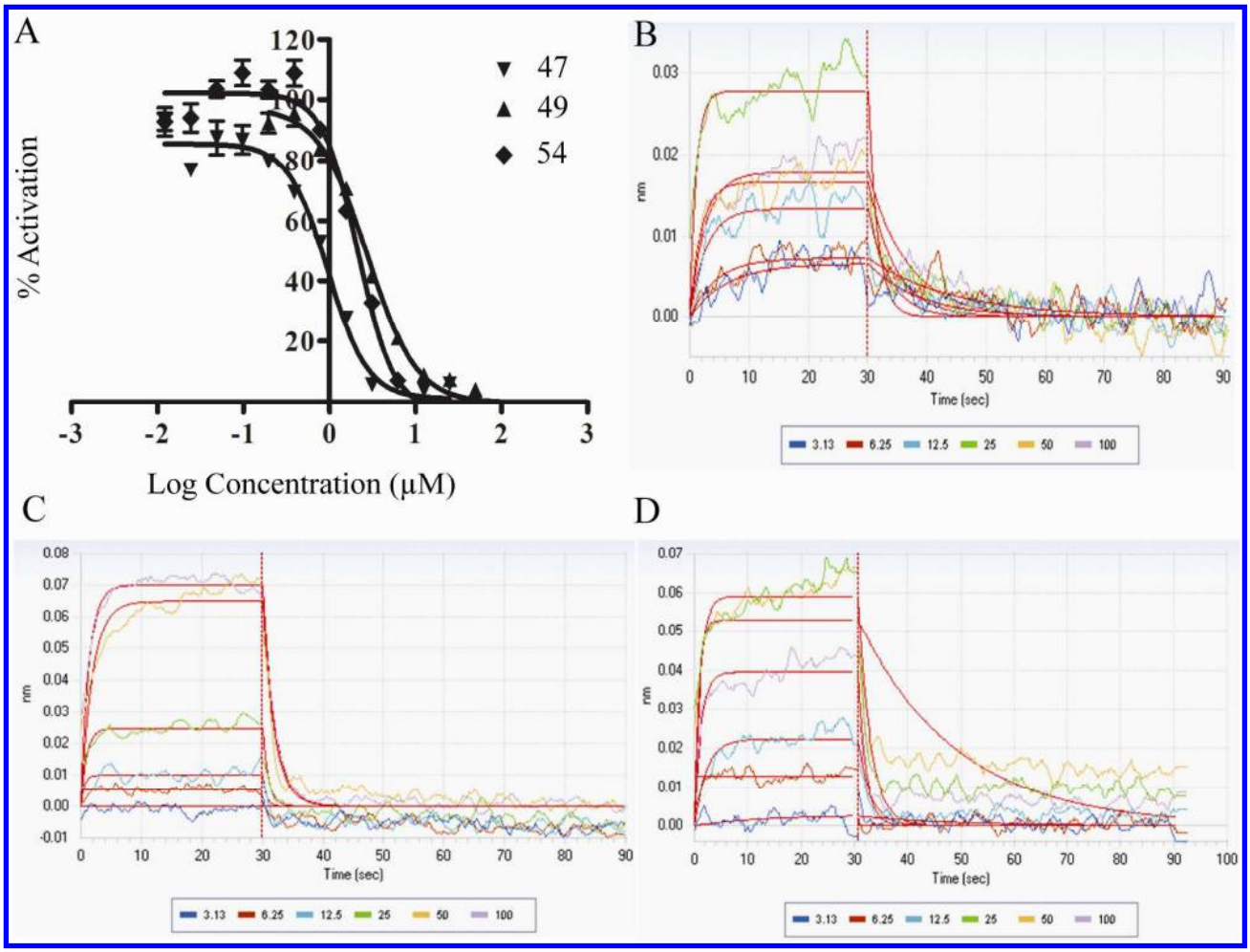

Figure 4. *A) Dose-response curves (0-100μM) illustrating the inhibiting effect of the compounds* ***47****,* ***49*** *and* ***54*** *on the AR transcriptional activity in cells. Data points represent the mean of two independent experiments performed in triplicate. Error bars represent the standard error of the mean (SEM) for n = 6 values. Data was fitted using log of concentration of the inhibitors vs % activation with GraphPad Prism 6.BLI dose-response curves (0-50μM) reflecting the direct binding of the compound B) compound* ***47*** *C) compound* ***49*** *and D) compound* ***54*** *to the AR LBD protein.*

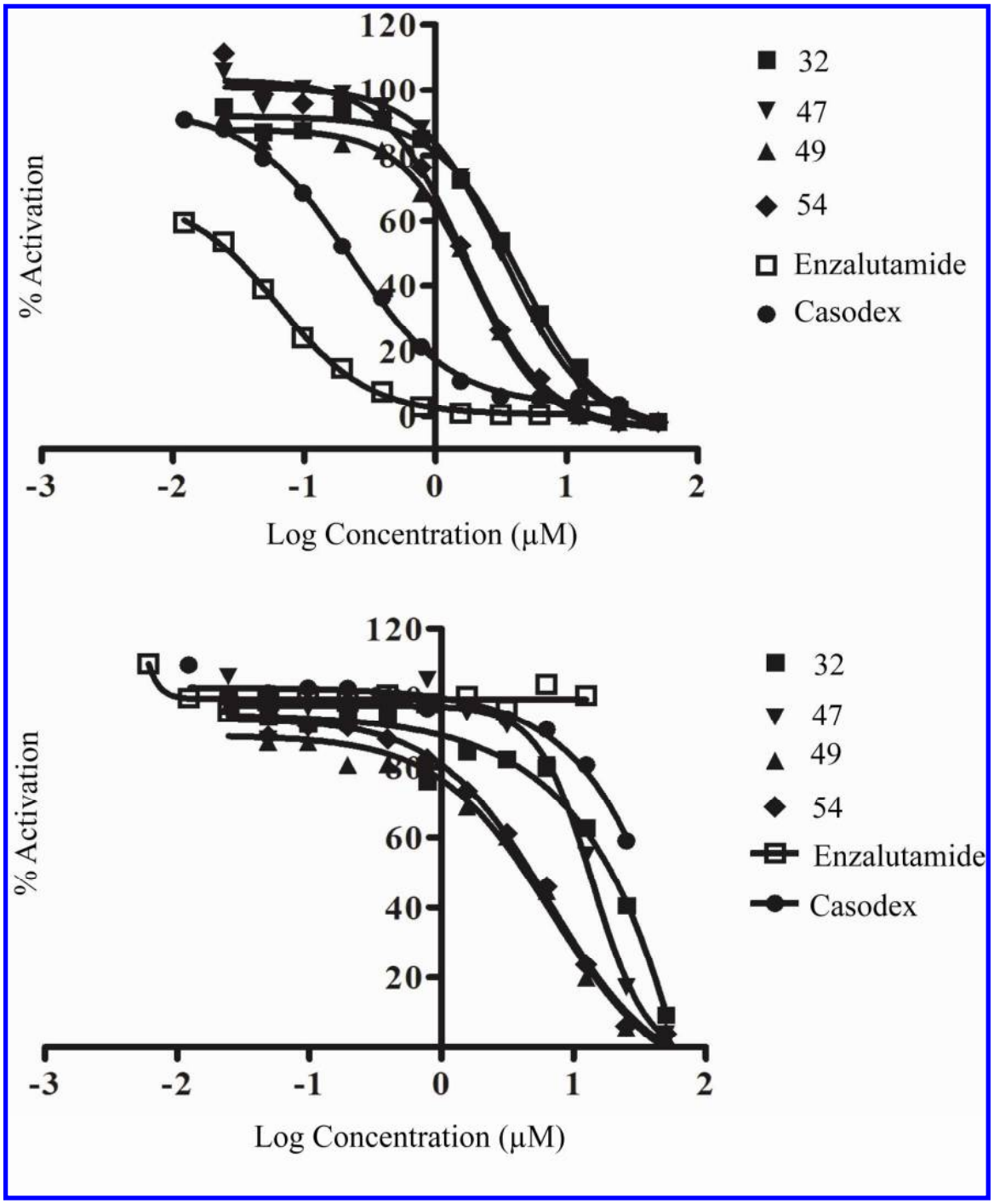

Figure 5. *Inhibition effect of* ***32****,* ***47, 49*** *and* ***54*** *in comparison to Casodex and Enzalutamide on PSA in dose response manner in A) LNCaP cells B) Enzalutamide resistant cells.*

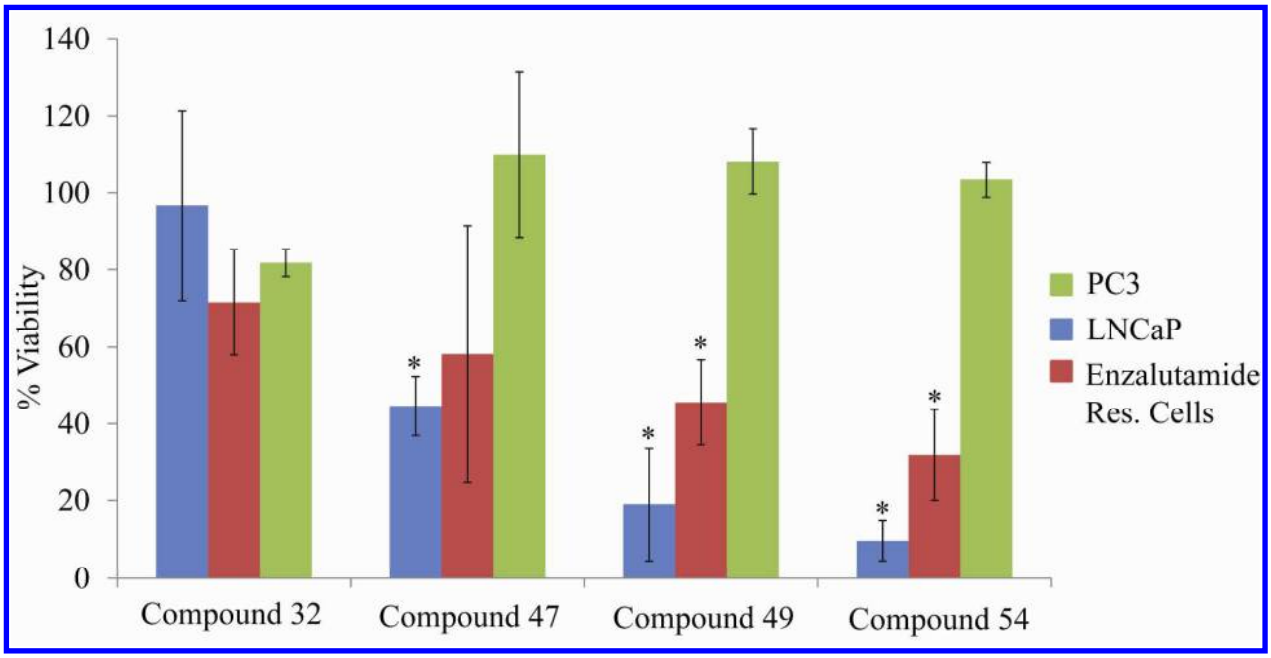

Figure 6: *The effect of compounds* ***32****,* ***47****,* ***49*** *and* ***54*** *on cell viability in LNCaP, Enzalutamide resistant cells and PC3 cells. % cell viability is plotted at 6μM concentration. Data are presented as Mean ± SEM. A p value <0.05 was considered very significant effect on LNCaP and Enzalutamide resistant cells compared with PC3 cells.*

TABLE OF CONTENT GRAPHIC